CARBON STOCK ESTIMATION USING VERY HIGH RESOLUTION SATELLITE IMAGERY AND INDIVIDUAL CROWN SEGMENTATION. (A CASE STUDY OF BROADLEAVED AND NEEDLE LEAVED FOREST OF DOLAKHA, NEPAL)

SAURAV KUMAR SHRESTHA
February, 2011

SUPERVISORS:
Dr. M. Schlerf
Dr. Y. A. Hussin

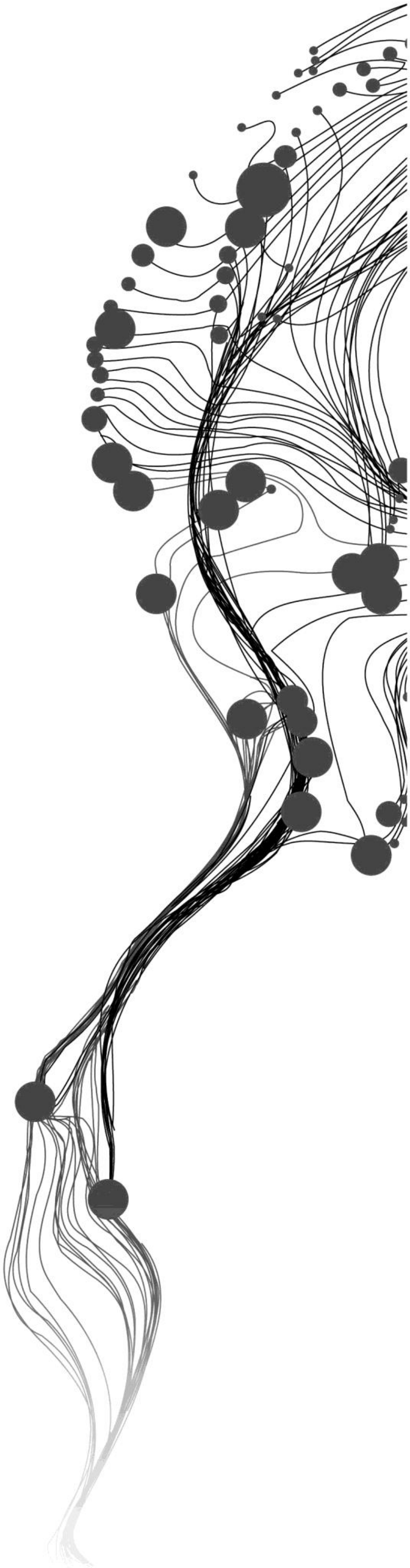

CARBON STOCK ESTIMATION USING VERY HIGH RESOLUTION SATELLITE IMAGERY AND INDIVIDUAL CROWN SEGMENTATION. (A CASE STUDY OF BROADLEAVED AND NEEDLE LEAVED FOREST OF DOLAKHA, NEPAL)

SAURAV KUMAR SHRESTHA
Enschede, The Netherlands, February, 2011

Thesis submitted to the Faculty of Geo-Information Science and Earth Observation of the University of Twente in partial fulfilment of the requirements for the degree of Master of Science in Geo-information Science and Earth Observation.
Specialization: Natural Resource Management

SUPERVISORS:
Dr. M. Schlerf
Dr. Y. A. Hussin

THESIS ASSESSMENT BOARD:
Prof. A. Skidmore (Chair)
Dr. Ir. J. G. P. W. Clevers (External Examiner, Laboratory of Geo-Information Science and Remote Sensing, Wageningen University)

ABSTRACT

There is a growing demand of precise and accurate estimation of carbon stock using remote sensing technology. The study, to estimate carbon stock, was initiated to develop a method based on the relationship of Diameter at Breast Height (DBH) and Crown Projection Area (CPA). It was carried out in a broadleaved and needle leaved forest using a very high resolution satellite image and object based image analysis.

The research design considered forest as a separate stratum from which two sample plots were randomly selected. The field data was collected together with the identification of at least ten trees from a plot. Various pre-processing of the image was done before giving it as input image to the ITC software. The segmentation process started with forest mask generation followed by valley following process. The valley following gave rise to the crown isolation process that resulted in distinct objects often referred to as "ISOLS".

The accuracy of crown segmentation was found to be 60% assessed in 1:1 correspondence with the under-segmentation and over-segmentation of 27%. It was found that 12% of the trees were missing where 81% accounted for broadleaved and 19% were needle leaved trees. The Root Mean Square Error (RMSE) in broadleaved and needle leaved trees were found to be 70% and 45% respectively. The classification accuracy obtained while classifying 3 species was 63% which improved to 81% when classification was done between broadleaved and needle leaved trees. Thus the high errors in the segmentation and classification led to weak DBH and CPA relationship for both broadleaved and needle leaved trees. It was found that result for broadleaved trees were poor compared to needle leaved, which was mainly attributed to segmentation problem *i.e.* over segmentation and under segmentation. Further, the location of the broadleaved trees in shaded region added to the poor classification and DBH - CPA relationship.

The ITC software could not give accurate segmentation that was needed to establish the relationship between DBH and CPA. The poor segmentation was observed more in the broadleaved than in the needle leaved trees.

ACKNOWLEDGEMENTS

This thesis would not have been possible without the guidance and help of several individuals who in one way or another contributed and extended their valuable assistance in the preparation and completion of this study.

First and foremost, I would like to express my sincere gratitude to my first supervisor Dr. Martin Schlerf for his innovative ideas, invaluable guidance, and support throughout the period. My heartfelt gratitude also goes to Dr. Yusif Hussin for his continuous support and motivation. Special gratitude also goes to Dr. Michael Weir, our course director, and his NRM team for the efficient management of this course.

The field works were only possible with the help of many people. I would like to thank Mr. Hammad Gilani and Eak B. Rana from ICIMOD for facilitating the field work very smoothly. I would also like to thank the chairman of the FECOFUN, Ms. Sita KC and former chairman Mr. Uddab Pokharel for their constant support in the field. Special thanks go to the facilitator Mr. Krishna Khadka, Ms. Anita Khadka and Mr. Naba R. Subedi. This appreciation in few words is not enough for you guys. I still remember the days that we started our field work very early in the morning and returned in the dark with the help of your mobile as light. Walking inside the dense forest without your help was next to impossible.

I would like to thank my entire colleague from NRM from all over the world. It was such a good experience working and sharing with you. Thanks to our CR, Dinesh Babu, for organizing the refreshments from time to time. Thanks to all Nepal carbon group especially Nandika who was my team member in Dolakha. Special thanks go to my NRM colleague from Nepal, Shyam, Rachana, Srijana and Upama. We always worked, studied, and discussed as a team. Moreover, we always helped each other. I can not express our unity in words. Thanks are also due to my entire Nepalese colleague whom I can not mention here one by one. You guys never let me think that I was away from home. It will be a memorable stay here in ITC in the days to come.

I am grateful to my well-wishers who helped me in giving comments and input in my thesis at the final stage when the time was like everything. Here, I would like to thank Hari B. Karki, Mandan Suwal. Dr. Raj B. Shrestha and Ms. Anita Joshi.

Finally, I would like to thank my beloved wife, Ms. Juleena Joshi, for support and encouragement. My three year old son, Saugat Shrestha, who always provided me some joy and energy to excel my study day after day. A special thought is devoted to my parents.

Saurav Kumar Shrestha
February 21, 2011
Enschede, The Netherlands

TABLE OF CONTENTS

LIST OF FIGURES

LIST OF TABLES

1. INTRODUCTION

1.1. Background

One of the reasons of global warming is caused by an excess of heat-trapping green house gases (GHG), for *e.g.* water vapour, carbon dioxide (CO_2), methane, nitrous oxides and ozone. Carbon dioxide is an important GHGs produced mainly by fossil fuel burning as well as change in land cover and land use (Dixon, 1994). In 1992, the United Nations Frame work Convention on Climate Change (UNFCC) was formed due to the concern of increasing amounts of GHGs that can influence global climate change. Similarly, in 1997, the Intergovernmental Panel on Climate Change (IPCC) was formed under the Kyoto Protocol to develop methodologies for estimating anthropogenic emissions by sources and removal by sinks.

Global forest covers around 30 per cent of the Earth's land surface (Dixon, 1994) and provide a significant standing stock of global carbon. Meanwhile, deforestation results in immediate release of carbon. It is estimated that global deforestation contributes to approximately 18 per cent of annual GHG emissions (Grainger, *et al.*, 2009). Thus they play an important role in stabilizing atmospheric concentration of CO_2 as they can switch between becoming sinks and sources depending upon succession, disturbances and management practices. (Masera, *et al.*, 2003). In 2007, Bali Action Plan (UNFCC, 2007) considered Reduction Emission from Deforestation and Degradation (REDD) as an important climate change mitigation action. The REDD concept is a provision of financial incentives to developing countries to reduce national deforestation. The developing countries not only receive the financial incentive but also join hand in combating climate change thereby conserving the biodiversity. (Gibbs, *et al.*, 2007). To participate in REDD, the countries signatory to UNFCCC, requires a robust method to estimate the amount of biomass and ultimately carbon stock. But the methods that have been adopted suffers from lots of uncertainties on accurate and precise estimates (Santilli, *et al.*, 2005).

1.2. Research Problem

Traditionally, carbon stock have been assessed using field-based inventory plots, that was expensive and time consuming (Asner, 2009). The application of remote sensing in carbon estimation made it possible to measure and monitor large areas lowering the cost and time.(Cohen & Justice, 1999; Hese, *et al.*, 2005). The rapid technological advancement and decreasing costs in the satellite and airborne mapping sectors are making carbon estimation more viable (Andersson, *et al.*, 2009; Asner, 2009).

Optical system, Synthetic Aperture Radar (SAR) system and Light Detection and Ranging (LIDAR) technology have been in widespread use for the estimation of carbon stock. Although the low cost and large swath width make them more appropriate (Fuchs, *et al.*, 2009), the low and medium resolution optical sensors have problems with atmospheric noise, mixed pixel and early signal saturation (Bottcher, *et al.*, 2009; Fisher, 1997; Lu, 2006). In addition the vegetation indices assessed from the low to medium resolution optical image do not provide significant correlation with biomass (Lu, 2005; Lu, 2006). SAR is considered better over optical sensors due to its 24 hours operation in all weathered conditions (Patenaude, *et al.*, 2004). However, SAR sensors have problem in signal saturation (Böttcher, *et al.*, 2008) and it is sensitive to surface topography that limits general application to flat or gently undulating terrain (Rosenqvist, *et al.*, 2003). At present, Light Detection And Ranging (LIDAR) technology is considered the best in providing the high accuracies of Above Ground Biomass (AGB) for standing tree species (Brandtberg*, et al.*, 2003). The lack of funding for satellite for LIDAR has caused the high cost of airborne platform. (Gibbs*, et al.*, 2007).

Despite the above mentioned limitations, the advent of a Very High Resolution (VHR) satellite image up to $1m^2$ like IKONOS, QuickBird, GeoEye and OrbView brought a reconsideration of the optical methods (Mallinis*, et al.*, 2008). Thus the VHR image motivated a shift from pixel based classification to object-based classification. In this classification, each object is composed of spatially adjacent pixels based on homogeneity criteria thus minimizing the problem of mixed pixel (Hay*, et al.*, 2005). The object based approach has limitations of over-segmentation and under-segmentation (Kampouraki*, et al.*, 2008). Over-segmentation occurs when one semantic object is partitioned into multiple smaller image objects while under-segmentation occurs when different semantic objects are grouped into one large image object. Thus, accuracy of segmentation is important as it also affects in classification (Asner & Warner, 2003). This approach converted a target of observation from forest stands into individual trees and subsequent analysis of species classification (Thomas, 2003).

The individual tree crown (ITC) segmentation software using the valley-following approach can be used to obtain crown information of broadleaved and needle leaved tree species (Gougeon, 2006). When the tree crowns are extracted accurately, the segmented crowns are converted into polygon termed as Crown Projection Area (CPA). The CPA measured on the field is the area of crown that is orthogonally projected on the ground. This segmented CPA is used to seek the relationship with field measured Diameter at Breast Height (DBH). DBH is considered as an important parameter that can be measured accurately on the ground, to estimate biomass using allometric equations. There have been several studies regarding DBH and crown width relationship (Smith*, et al.*, 1992). However, the relationship of DBH and CPA are scarce (Krajicek *et.al* (1961) as cited in (Shimano, 1997). Shimano (1997) studied DBH and CPA relationships for deciduous and coniferous trees in sample cohorts and found significant relationship between DBH and CPA. The relationship is dynamic because in nature there is always competition between neighbouring trees and it increases upon reaching to canopy closure (Shinozaki*, et al.*, 1964). Due to this dynamic nature the relationship varies. Shimano (1997) developed Linear regression model, Second power functional model, Logistic function model and Power sigmoid model.

Asner *et.al,* (2002) focused on developing accurate model for estimation of crown dimensions using high resolution satellite imagery. Studies show that there exists a relationship between DBH and CPA and there are very few researches done related to the tree crown (Hemery*, et al.*, 2005). Since, there has not been any study carried out to estimate the carbon stock from CPA, this research will fill the gap that remains in the scientific domain of crown area to estimate the carbon stock using VHR satellite image.

1.3. Objective

The overall objective of this research is to develop a method to estimate Above Ground Carbon (AGC) stock of broadleaved and needle leaved tree species using a very high resolution satellite image and object based image analysis. The specific objectives, research questions and hypothesis are presented in Table 1.

Table 1.1 Specific objective, Research Questions and Hypothesis

<table>
<tr><td colspan="2">Specific Objective 1: To identify the segmentation accuracy of the ITC software</td></tr>
<tr><td>Research Question</td><td>Hypothesis</td></tr>
<tr><td>1.1 What is the overall accuracy of segmentation using ITC software?
1.2 What is the accuracy in broadleaved trees and needle leaved tree species?</td><td></td></tr>
<tr><td colspan="2">Specific Objective 2: To identify the accuracy of species classification</td></tr>
<tr><td>Research Question</td><td>Hypothesis</td></tr>
<tr><td>2.1 Are the dominant trees in the study area separable from each other?
2.2 What is the overall classification accuracy of dominant trees?</td><td></td></tr>
<tr><td colspan="2">Specific Objective 3: To identify the relationship of CPA-segmented with DBH and CPA-segmented with carbon for broadleaved and needle leaved tree species</td></tr>
<tr><td>Research Question</td><td>Hypothesis</td></tr>
<tr><td>3.1 Is there any relationship between CPA-segmented with DBH and CPA-segmented with carbon for broadleaved and needle leaved tree species and how strong is the relationship?</td><td>3.1 Ho: There is no relationship between CPA-segmented with DBH and CPA-segmented with carbon and CPA-segmented responds DBH with low R^2 for both broadleaved and needle leaved tree species.

H1: There is significant relationship between CPA-segmented with DBH and CPA-segmented with carbon and CPA-segmented responds DBH with high R^2 for both broadleaved and needle leaved tree species</td></tr>
<tr><td colspan="2">Specific Objective 4: To Develop linear regression model to estimate above ground carbon for broadleaved and needle leaved tree species.</td></tr>
<tr><td>Research Question</td><td>Hypothesis</td></tr>
<tr><td>Does the linear regression model accurately estimate above ground carbon in broadleaved and needle leaved forest?</td><td>4.1 Ho: Low R^2 and RMSE > 30%
4.2 H1:High R^2 and RMSE $\leq$30%</td></tr>
</table>

Specific Objective 5: To evaluate the processing steps in estimating carbon from very high resolution satellite image.	
Research Question	**Hypothesis**
5.1 What is the RMSE between visually delineated crown diameter and crown diameter of the tree measured in the field? 5.2 What is the RMSE between CPA-segmented and CPA-visual? 5.3 Is there any relationship between CPA-visual and DBH and how strong is the relationship for both broadleaved and needle leaved tree species?	

2. MATERIALS AND METHODS

Chapter describes materials and methods used in the study which begins with the brief description of the study area. The materials and the software used in the study are also described. Finally, in the methods, a flow chart explains the overall workflow.

2.1. Study Area

2.1.1. Location

Charnawati, watershed, is located in the Dolakha district of the Central Development Region of Nepal. The geographic location of the watershed is 27^0 55' 02" N to 27^0 59' 43" N latitude and 84^0 33' 23" E to 84^0 40' 41" E longitude (Figure 2.2). The altitude of the study area ranges from 835 m to 3549 m and spreads over 14036 ha (ICIMOD, 2010). The motivation for selecting the study area was due to the presence of both needle leaved as well as broadleaved forest due to the altitudinal variation.

2.1.2. Topography

The topography of the district is characterized by high Himalayas and high mountain physiographic region where the 30% land is under the slope (DDC/LGP, 1999).

2.1.3. Climate

The watershed has average rainfall of 2232 mm and most of the rainfall occur during the monsoon *i.e.* during June-September (Bista, 2000). The maximum average temperature is 20^0C during the months of mid-April to mid-Sept and the minimum average temperature is 8^0 C in the cold months of December and January.(ICIMOD, 2010). The climate of the watershed varies from sub-tropical to sub alpine zones with diverse vegetation(DDC/LGP, 1999).

2.1.4. Vegetation

The vegetation cover of the watershed is rich and comprised of needle leaved tree species and mixed broad-leaved forests (Figure Figure 2.1). *Pinus roxburghii*, Pinus wallichii, Pinus patula. *Rhododendron arboreum, Quercus semicarpofolia, Alnus nepalensis*, and *Schima wallichii* the dominant species. The common associated species, of middle hills of central of Nepal, like *Shorea robusta* and Schima-castonopsis forests are also found in the lower altitudes. The three Pine trees *i.e. Pinus roxburghii, Pinus wallichii* and *Pinus patula,* with conical shaped crowns, are referred hereafter as needle leaved tree species. Similarly, *Alnus nepalensis* (referred hereafter as Alder trees) and *Schima wallichii* together with many other broadleaved trees, having oval or rounder shaped crowns, are called as broadleaved trees.

There are 58 Community Forests User Groups (CFUGs) with the total forest area of 5996 ha. in the watershed. CFUG is an autonomous institution, registered in District Forest Office (DFO), and solely responsible for the management of Community Forests (CFs).

Figure 2.1 Mixed broadleaved and needle leaved trees

There are five types of land cover in the watershed that is presented in Table 2.1.

Table 2.1 Land cover types of the watershed

Land cover type	Area (ha.)	Percentage
Total forest of the watershed area (all types of forests)	7492	53.38
Water bodies	1	0.01
Bare Soil	629	4.48
Grassland and degraded forest	204	1.45
Agriculture Land and built-up areas	5710	40.68
Total	**14036**	**100**

Source: (ICIMOD, 2010)

2.1.5. Subset of the study area

A study area of size 297 ha. consisting of 12 CFUGs was defined to account as study area due to the processing time required by the segmentation software. The CFUGs were selected on the basis of proportional distribution of broadleaved and needle leaved tree species. The adjoining CFs were selected so that total area did not exceed more than 300 ha (Appendix 3).

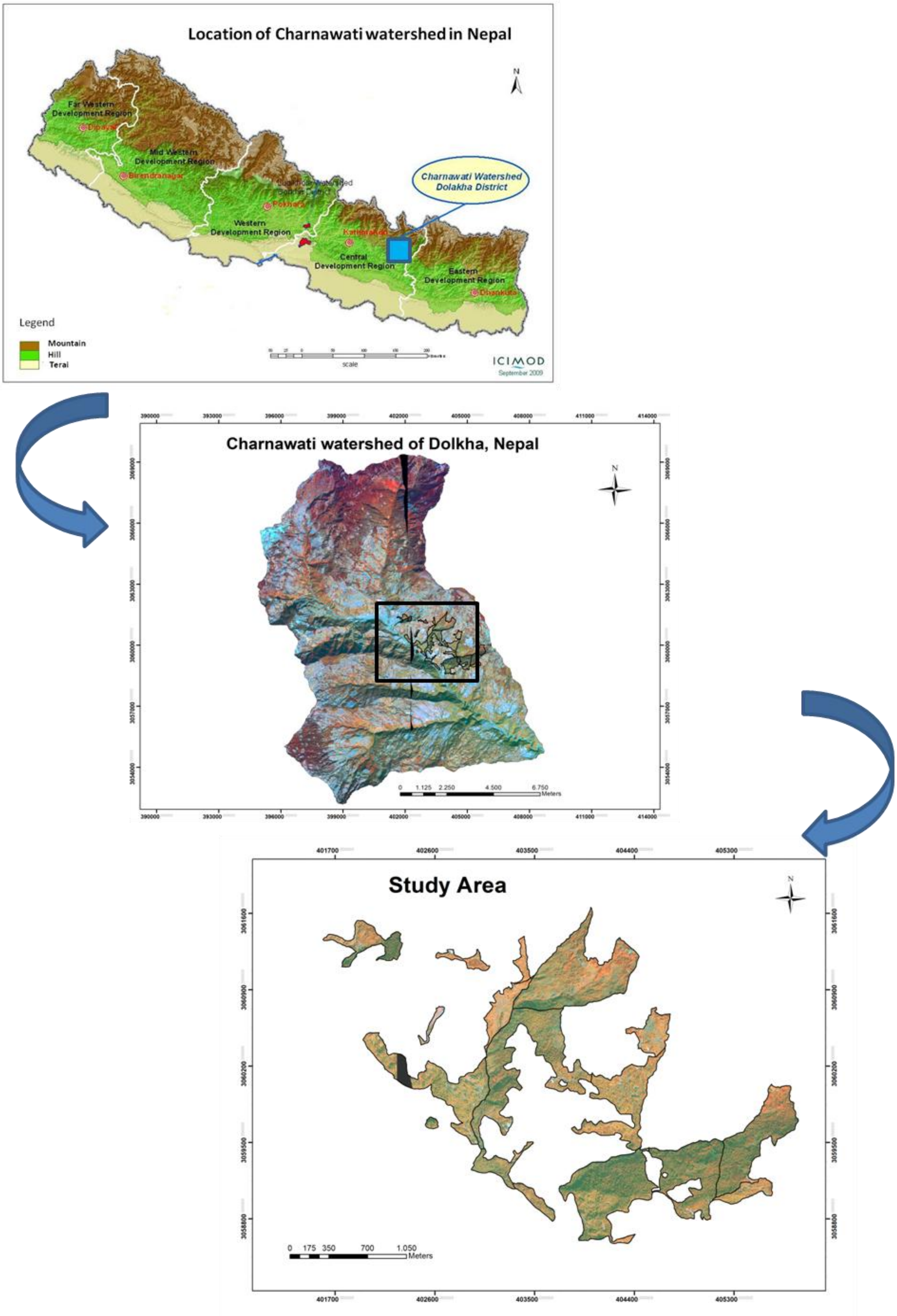

Figure 2.2 Location of study area in Charnawati watershed Dolakha, Nepal

2.2. Materials

2.2.1. Satellite Data

The GeoEye images, multispectral resolution of 2m and panchromatic image of 0.5m resolution, were used in the study. The multispectral image has 4 bands that include 3 bands in the optical domain and one band in Near Infra-Red (NIR). There are three types of GeoEye imagery products for *e.g.* Geo class, Geo Professional and Geo Stereo. It is 11 bit image and belongs to Geo product class. The Geo Product is a radiometrically-corrected image (GeoEye, 2011). The product can be orthorectified by the users using digital elevation model (DEM) together with ground control points. The panchromatic and multispectral images of the study area were captured in November 02, 2009. The time of image acquisition was 10.00 am (local time) and the season was late autumn. The Sun elevation angle at the time of collection was 46^0 and view angle was 25^0 from nadir. The shape file of boundary of the watershed, boundary of the CF and topographic maps were also used in the study.

2.2.2. Software

The list of the software and its purpose are presented in Table 2.2

Table 2.2 List of software used in the study

Software	Purpose of use
Erdas Imagine 2010	Image fusion to get pan-sharpened image. Image subset, Image filtering, Assessment of classification accuracy.
ArcGIS 10	Map production, Generation of random points, Visual crown delineation of the identified trees, Data partitioning, Conversion of raster image into polygon shape format *etc.*
Individual Tree Crown (ITC) suite PCI V 9.1	Segmentation of the tree crown
eCognition	Classification of the segmented crown ISOLS
Java Technical Suite	Assessment of Segmentation Accuracy
SPSS 16.0	Data Analysis, Chart
Microsoft Excel 2010, XLSTAT 2010	Data Analysis, Chart
Microsoft Word	Thesis Writing
Microsoft Visio	Construction of flowchart
Power point	Presentation

2.3. Orthorectification and Pan-sharpening

The orthorectified multispectral and panchromatic images using DEM (*i.e.* of 2m accuracy) was obtained from International Centre for Integrated Mountain Development (ICIMOD) project in Nepal. The image had some distortion or artefact after the ortho-rectification especially at very steep slopes. The multispectral image of 2m resolution (4 bands) was fused with panchromatic image of 0.5 m resolution to get a pan-sharpened image of 0.5m resolution using IHS (Intensity, Hue, Saturation) technique. The IHS technique was used in order to retain n the spectral signatures of the input colour image and spatial features of the input pan image. The product of the fusion was 3 bands pan sharpened image where blue band was discarded forming NIR, Red and Green bands image combination.

2.4. Research Design

2.4.1. Sampling Design

The research design was made considering each CF as a separate stratum. This was done in order to ensure that strata spread over the whole Charnawati watershed. Further, two sample plots following Cochran & Dalenius (2006) of 500m2 (Husch*, et al.*, 2003) were selected randomly from each stratum making a total number of 116 sampling plots. The dataset of 48 sample plots that had additional information of field crown diameter, measured in July 2010 by ICIMOD was used. The sample plots to be collected was then reduced to 75 sample plots. The details of the sample plot information can be seen in the Appendix 2.

2.5. Method flow chart

The method flow chart is mainly divided into three components as shown in different colour boxes (Figure 2.3). The tasks and output of the field measurements is shown inside the green box. Similarly, the remote sensing and GIS works are shown in the blue box. Finally, statistical analysis including the model development is depicted within the purple box.

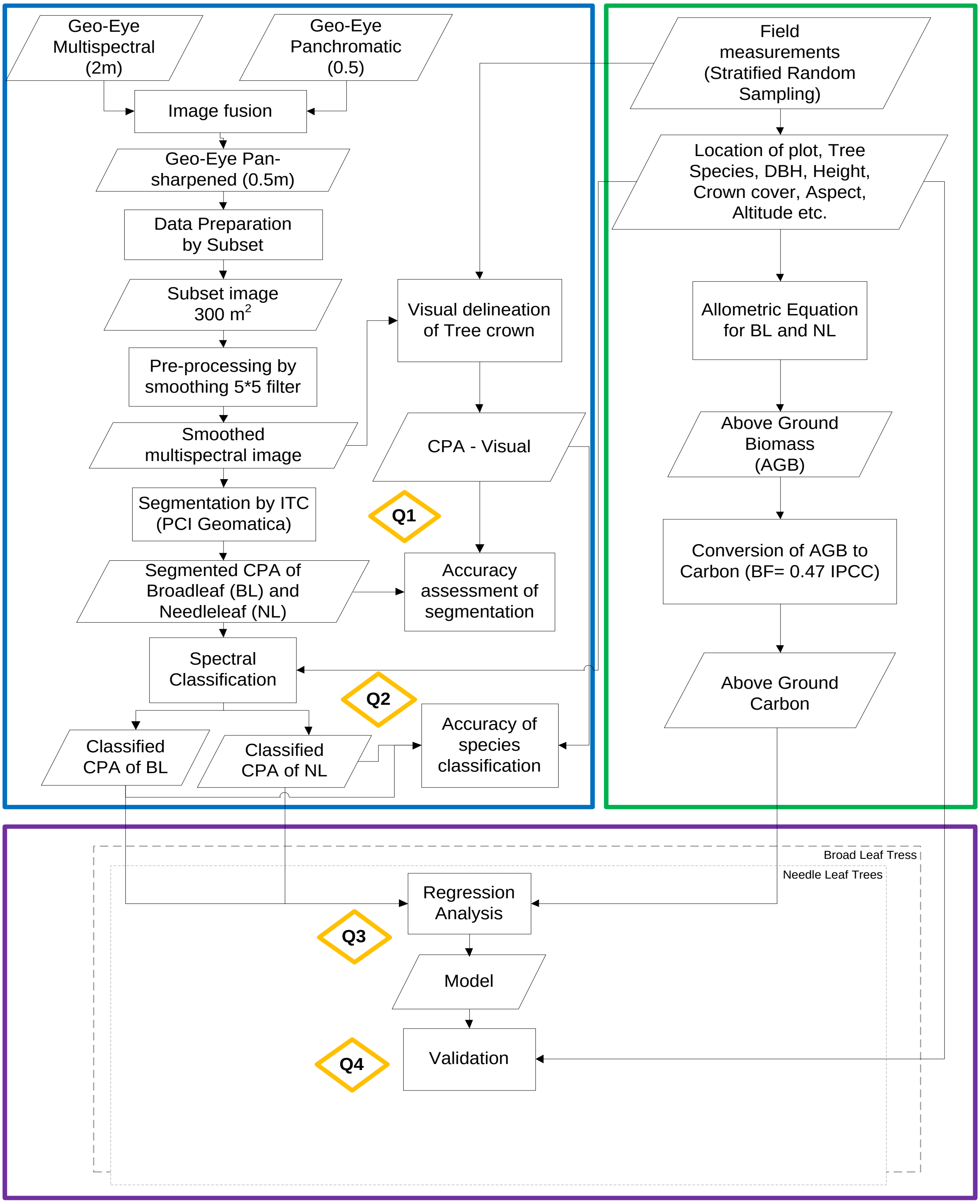

Figure 2.3 Flow chat of the research method

2.6. Field Work

The enlarged tree identification maps were prepared before the field work where a buffer of 500m² (radius 12.6m) was created for all the circular sample plots considering the points as centre of the plot. The map was prepared for each plot in the 1:1000 scale where a single tree can be seen [Figure 2.4(a)].

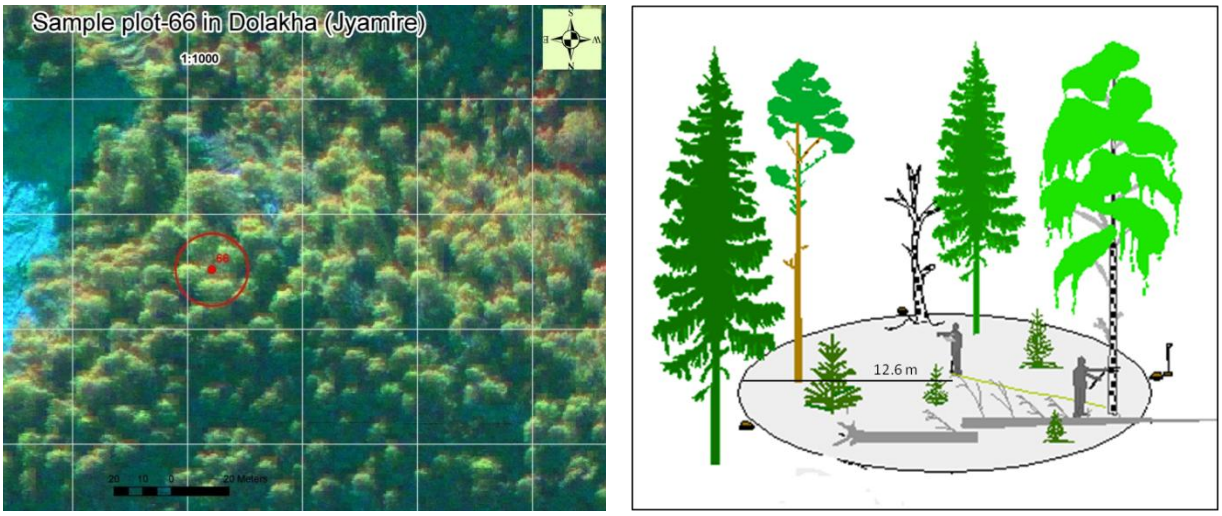

Figure 2.4 (a) Enlarged map (1:1000) with buffer 500 m2 (b) Circular plot and measurement (Source modified from Integrated monitoring system 2011, Sweden)

Plot centres were located using Ipaq, GPS and visual interpretation of the enlarged map [Figure 2.4(a)] to ensure the location of plot in the field with corresponding plot on the map. The circular plot of radius of 12.6 m [Figure 2.4 (b)] was laid (Husch*, et al.*, 2003). The radius of 12.6 m was adjusted in the slope using slope correction factor (A. de. Gier 2003: ITC lecture note). For each plot, the coordinate, canopy cover, aspect, altitude and underground flora were recorded in the recording sheet. All trees that were above 10cm Diameter at breast height (DBH) were selected for measurement as it is assumed that small trees (below 10 cm diameter) contribute negligible amount of biomass (Brown, 2002). All the trees in the plot were identified, DBH and height were measured. It is recorded in the recording sheet. Further, at least ten trees (among the measured trees) were identified on the map using the shapes of surrounding objects such as trees, trails, agriculture land, river, landslide, shadows and rocks. Identification of the trees (apart from dead and crown overlapped) was carried out as the tree crowns were visible almost in the same direction and distance from each other. The trees were also identified outside of the plot and their DBH, height and species were recorded. Field measurements confirmed to standard forest mensuration methods (Brack, 2004; Verplanke & Zahabu, 2009). The research team could measure only 64 plots in the study areas out of the 75 sample plots that were planned.

2.7. Visual delineation of tree crown

Figure 2.5 and Figure 2.6 shows the tree crown taken from above and below the tree. The captured image consists of tree crown, understory vegetation, and bare soil. This gives rise to the first step which was to separate tree crowns from their background. The image was smoothed using low pass filter of 5*5 in pan-sharpened multispectral image as well as panchromatic image. The visual delineation of identified trees were carried out at 1:100 to 1:200 scale visualizing in all the original IHS image, smoothed panchromatic image and smoothed pan-sharpened image. The visually delineated crowns were used to evaluate the segmentation. Besides, it was also used in species classification and accuracy assessment.

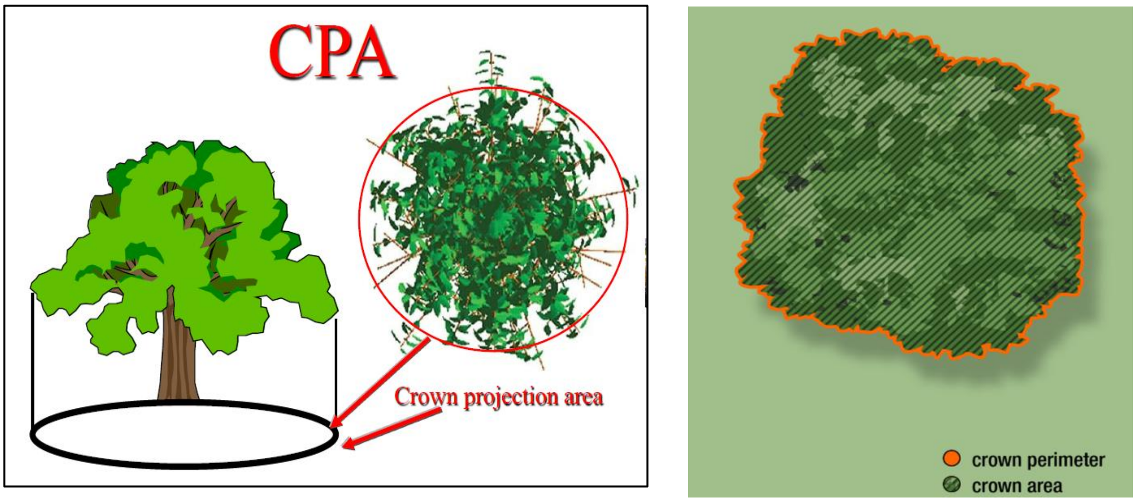

Figure 2.5 (a) Crown Projection Area (CPA) in the ground (b) CPA from above [After Gschwantner, (2009)]

Figure 2.6 Tree crown from below the tree (a) Needle leaved tree crown (b) Broadleaved tree crown

2.8. Segmentation of the image

Individual Tree Crown (ITC) is an integrated software package and works under the PCI Geomatica environment. The ITC suite uses semi-automatic technique to extract individual tree crown captured by high resolution airborne or satellite imagery. The software is based upon following the valley of shade that is present in between the tree crowns of high resolution image (Gougeon, 2006). Each process of segmentation was explained using illustrated area demarcated by a box (Figure 2.7)

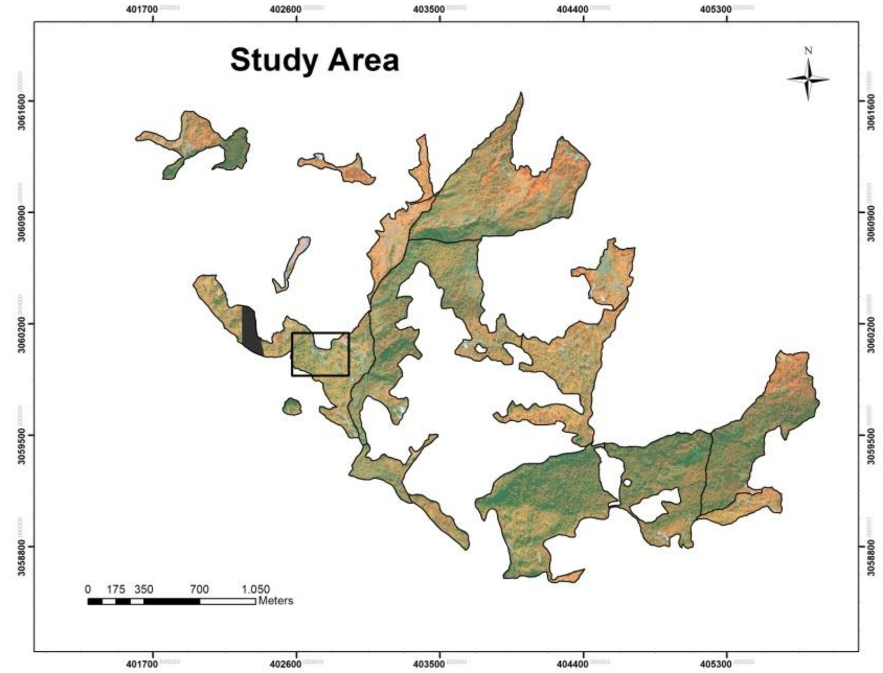

Figure 2.7 Illustrated area demarcated by box

2.8.1. Data preparation for segmentation

Subset of the study area was made from pan-sharpened image in Erdas. The 5*5 low pass filter was used to smooth the image as the 0.5m resolution images show a lot of variation within one canopy. The smoothing filer would reduce the variation and make the task easy for segmentation.

2.8.2. Mask out of non-forested areas

Elimination of non-forest areas (*e.g.*, roads, man-made features, agriculture/pasture areas, rivers, lakes *etc*..) was a pre-requisite process in order to avoid software to be crashed (Gougeon, 2010b). The algorithm of non forest mask works by detecting pixels that have small infra-red radiances compared to that of mean visible radiances (NIR < visible) (Gougeon, 2010b). The process started with selecting NIR band as illumination channel as it is sensitive to illumination variations and has good response to vegetative materials(Gougeon, 2003). Further, NIR and visible channels were normalized by average grey level (called as Navg) under the non-vegetation comparison criteria selection. The process resulted in the bitmap *i.e.* mask of non-forest areas.

2.8.3. ITC Valley Following

ITC Valley Following (ITCVFOL) is based on the concept that the high spectral values on bright tree crowns and lower values between the shaded areas of tree crowns form peaks as mountains and valleys of shade (Leckie*, et al.*, 2003). The process started with giving forest mask as input image together with the selection of illumination image (NIR). There are three important thresholds *viz.* local maxima (upper threshold), local minima (lower threshold) and valley noise which were given in threshold generation mode manually. Local minima were estimated from the edges of the tree crown, shaded sides of tree crown and shaded surrounding areas. Similarly, local maxima were assessed by checking the reflectance values from bright areas of tree top. The third valley noise threshold was given according to the radiometric resolution of the image. The valley following algorithm in the lower thresholds worked setting lower threshold which considered any pixel value below this as valley of shade (Leckie*, et al.*, 2003). Additionally, the algorithm in the local maxima was made in such a way that any shade in between the very high radiance values of tree top is ignored and it was meant to prevent the breaking of a single tree crown (Gougeon, 2006). This upper threshold was especially important for a very big crowns or species having star like crown (Gougeon, 2003). Also, the third threshold called as valley noise threshold was used to measure the radiometric instability. The local minima, local maxima and valley noise were given as 460, 1015 and plus minus 3 respectively. Figure 2.8 shows the output of the valley following approach in which brighter points are seen as peak which is top of the tree and blue lines as valleys *i.e.*. boundary of the tree crown.

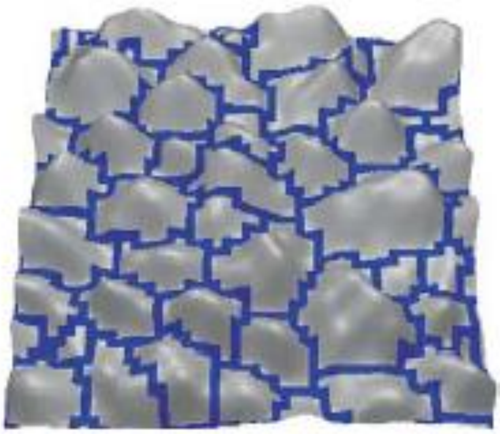

Figure 2.8 Valley following of shade in blue colour separating tree crown (Source: Culvenor 2004)

2.8.4. ITC Isolation

All the tree crowns were not separated during the valley following process. It was because the crown as well as branches often overlapped each other (Gougeon, 2010a). Rule based process ITC isolation was used in order to overcome the overlapping of the tree crown (Leckie*, et al.*, 2003). The algorithm for the crown isolation works following the crown boundaries favouring clockwise and finally delineating closed shapes (Gougeon, 2003). The partially separated tree crown from ITC Valley following bitmap was given as input segment and forest type was set to mature. The process produced distinct objects often referred to as “ISOLS” in the bitmap format.

2.8.5. Segmentation Accuracy

There are several methods to assess the accuracy of segmentation (Zhang, 1996). However, two methods were mainly considered for the tree crown accuracy assessment when the visual delineation and automatic segments were available (Clinton*, et al.*, 2010). One of the method is called Relative Area developed by Moller (2007) and other is called as 1:1 correspondence developed by Yang (1995). Out of the two methods 1:1 was chosen to assess the accuracy as this method has been in widespread use for tree crown. .

One to one correspondence relied on observation of 1:1 matching of polygons between visual delineation and automatic segments. The 1:1 correspondence was carried out to see the accuracy by visual interpretation. This method can provide the segmentation accuracy for both broadleaved and needle leaved tree species. In addition it also provided the information of missing trees. The criterion (Figure 2.9) was set such that here was at least 50% overlap between visual delineation and CPA segments (Zhan*, et al.*, 2005). The number of good matches provided the accuracy of this method. Over-segmentation and under-segmentation, being a complex procedure, were not dealt separately. However, the overall segmentation problem (both over-segmentation and under-segmentation) of both broadleaved and needle leaved tree species was calculated by subtracting the good matched and missing tree from the total tree. The output of the 1:1 correspondence was also used in the classification, looking at DBH-CPA relationship and model development.

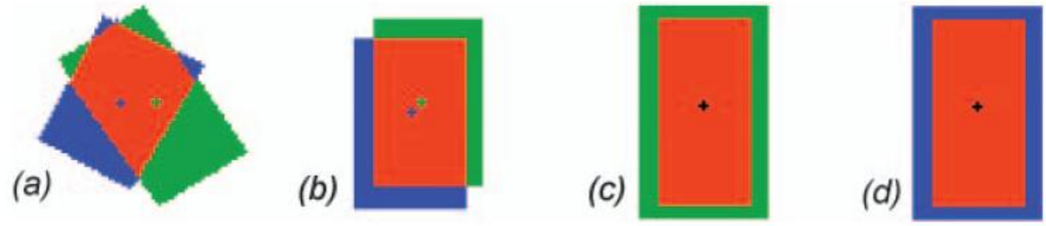

Figure 2.9 Four matched Cases of extracted objects (matched region is shown in orange:; green indicated an visual delineation; blue automatic segments (a) More than 50% match; (b) Visual and automatic segments are same but differ in position (c) and (d) an extracted reference object matches with the same position but differ in position.. (Source: Zhan *et.al* 2005)

2.8.6. Classification of Segmented tree crown

The accuracy for the automatic-segmented crown delineations (CPA-segmented) and classification (recognition accuracy) was assessed in eCognition using nearest neighbourhood supervised classification. The classification could not be carried out in ITC as it was complex due to the mixed forest of the study area and it was best suited for plantation and clustered trees of the same species (Gougeon, 2010b). The visually delineated tree crowns, which were used for the classification, were partitioned into 60%-40% for training and validation data. The classification was initiated by training and building up a knowledge base for the classification and this knowledge base is called class hierarchy (Baatz, 2004). The reflectance curve was made for the dominant species in the study area in order to see the separability amongst the tree species. The classification was carried out in 3 class *viz.* dominant needle leaved Pine trees, dominant broadleaved Alder trees and Broadleaved Schima wallichii and other broadleaved trees grouped as others. Again the classification was done with two classes of broadleaved and needle leaved tree species for which the model will be developed for broadleaved trees and needle leaved tree species. The classification accuracies were assessed in Erdas 2010 for both the 3 classes and two classes.

2.9. DBH-CPA relationship and development of Linear Regression Model

2.9.1. Above Ground Biomass calculation

The biomass includes both AGB and below ground biomass *viz.* leaves, roots, seeds, and stalks *etc.* Brown (1997) defined biomass as the total amount of above ground living organic matter in trees expressed as oven-dry tons per unit area. AGB is usually the mass of the above ground portion of live trees mainly the stem, branches and foliage (Brown & Lugo, 1992).

The allometric equations of broadleaved and needle leaved tree species of India having similar pattern of precipitation and altitude were used since oven dry allometric equation for Nepal was not available. The

AGB was calculated using allometric equations based upon the DBH and tree height both of which were measured in the field. The following allometric equation (1) by Chave *et.al* (2005) was used to calculate biomass for broadleaved trees as it was developed for moist forest where the precipitation is around 2000m and altitude is more than 1000m. This allometric equation used both DBH and Height information together with wood density. The wood density was used from Nepalese broadleaved trees (ICIMOD, 2010).

$$Y=0.0509*P\,(DBH)^2*H \tag{1}$$

Where, Y=Biomass,
P=Wood density which is 0.594 (for broadleaved trees)
DBH = Diameter at breast height and
H=Height

Similarly, the allometric equation (2) prepared by (Chaturvedi, 1982) was used to calculate the biomass for needle leaved tree species. The equation was developed for *Pinus roxburghii* and it considers the biomass of stem, branches and foliage. It was used to calculate the AGB of needle leaved tree species as *Pinus roxburghii* in India and Nepal grow in similar situations.

$$LnY=a+b*LnX \tag{2}$$

Where, Ln Y = Natural log of Biomass,
a = intercept
b = Slope
Ln X = Natural log of X

The biomass thus obtained from the allometric equation was converted into carbon using conversion factor (0.47) (IPCC, 2003) as shown below.

$$C=B*C.F$$

Where, C= Carbon stock (kg.)
B= Dry Biomass (kg.)
C.F. = Carbon fraction of biomass (0.47)

2.9.2. DBH-CPA relationships for broadleaved and needle leaved tree species

The relationship between DBH from the field and CPA from the segmentation was assessed in linear regression at confidence interval of 95 %(α=0.05) for both broadleaved trees and needle leaved tree species. Only the good matched trees obtained from the 1:1 correspondence Table 3.3) were used to seek the relationships. The correlation coefficient (R), coefficient of determinants (R^2) was calculated.

2.9.3. Development of Linear Regression Model

After seeking the DBH-CPA relationship the data was partitioned in 70-30 (train-validation) for model development. The linear regression for test was carried out where CPA from the segmentation was placed in X-axis (independent variable) and Carbon in Y-axis (dependent variable) since the carbon was sought to be derived from CPA. In general, a high R^2 or a low RMSE value often indicates a good fit between the model developed and the sample plot data. The R^2 and RMSE (together RMSE%) was calculated to see how accurately the model predicted the carbon with respect to the measured carbon from the field. It was carried out 10 times and R^2 and RMSE was averaged and the model was chosen. Similarly the data set aside for validation was also regressed in the same manner for 10 times to validate the model. The RMSE and RMSE % were calculated. The R^2 from the train and RMSE% from the validation was used to assess the strength of the model. The RMSE was calculated using the formula below;

$$RMSE = \sqrt{\frac{1}{n}\sum_{i=1}^{n}(x1_i - x2_i)^2} \qquad (3)$$

Where, RMSE = Root Mean Square Error

X1i = Measured carbon in the field
X2i= Estimated carbon from the model
n= no. of observation

2.10. Evaluation of the steps of processing

There might be several errors occurring in each step from the high resolution images that can affect the accurate carbon estimation. There might be errors in visual delineation although it was done carefully at 1:100 and 1:200 scale (Leckie, *et al.*, 2005). So, the verification of visual delineation was carried out by comparing it with the crown diameter that was measured in the field. The crown diameter of the trees in the image was obtained from ArcMap. In the ArcMap one of the sides of crown (longer or shorter) was measured and another one was measured in perpendicular to the first one. It was averaged to extract the crown diameter of the image. The secondary data of 48 sample plots were used for verification. The 10% of the visually delineated crown were selected randomly and Root Mean Square Error (RMSE) was calculated using equation (3). One to one relationship was also plotted in the chart to see the difference.

Although, 1:1 correspondence was used for measuring accuracy, it can introduce subjectivity. It is because sometime it is difficult to distinguish whether the overlapping between the CPA-segment and CPA-visual is 45% or 50% to account for good match. Hence, the evaluation of accuracy assessment by calculating RMSE between CPA-visual and CPA-segmented can be a good one. So, RMSE of the CPA-segmented with respect to the CPA-visual was calculated using equation (3) for both broadleaved and needle leaved tree species. It was done since the problem of over-segmentation and under – segmentation persist in the segmentation process. If the error was very high it can affect in the accurate estimation of carbon. The one to one relationship was also carried out by plotting CPA-segmented and CPA-visual in the scatter plot.

Good crown segmentation can result in good CPA and DBH relationship. The CPA-visual and DBH relationship was also carried out in order to retrieve the actual relationship. By doing this, it could be known whether there exists relationship or not.

3. RESULTS

3.1. Descriptive Statistics

The descriptive statistics of DBH, height for both broadleaved and needle leaved tree species is presented in Table 3.1 and Table 3.2. The DBH of broadleaved trees have mean and standard deviation of 19cm and 4.41 cm respectively. Similarly, the height of the broadleaved trees has mean and standard deviation of 14m and 2.63m respectively (Table 3.1).

Table 3.1 Descriptive statistics of broadleaved tree species

Attributes	Minimum	Maximum	Mean	Std. Deviation
Height	8	17	14	2.63
DBH	13	26	19	4.41

The mean and standard deviation of DBH for needle leaved trees was found to be 26cm and 5.02cm respectively. Similarly, mean and standard deviation of height of the needle leaved trees was 17m and 2.69m respectively (Table 3.2).

Table 3.2 Descriptive statistics of needle leaved tree species

Attributes	Minimum	Maximum	Mean	Std. Deviation
Height	13	20	17	2.69
DBH	19	33	26	5.02

3.2. Visual delineation of tree crown

The smoothing of both of the images (pan-sharpened multispectral and panchromatic image) using 5*5 averaging filter was found to be effective as edges of the crown could be differentiated from the background (Figure 3.1 a, b and c). Edges of the crowns that were overlapped were also distinguishable when zooming at 1:100 scales. The smoothed panchromatic image provided better visual interpretations when the crowns were overlapped (3.1 c). Although 1120 tree crowns were delineated only 170 trees were used in the study.

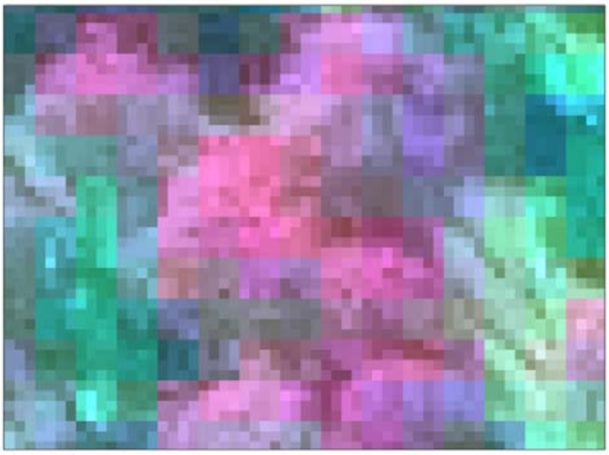

(a)

(b)

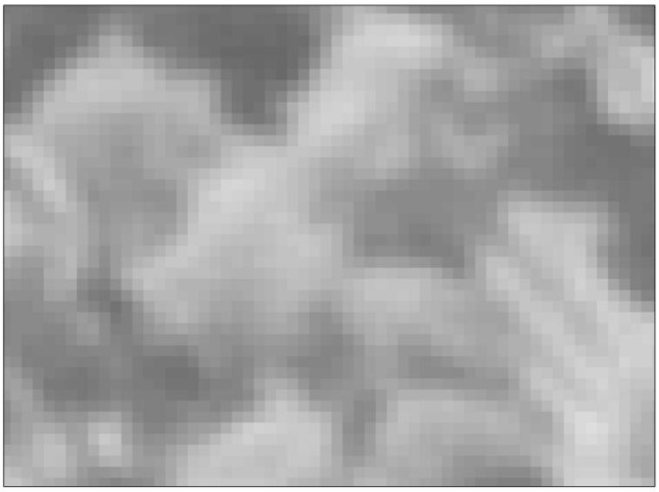

(c)

Figure 3.1 Pre-processed image for illustrative purpose at 1:150 scale (a) Pan-sharpened image, (b) 5*5 Smoothed pan-sharpened image and (c) 5*5 smoothed panchromatic image

3.3. Result of Segmentation

The non-forest mask was produced as a bitmap that can be seen in the illustrated as blue colour [Fig 3.2 (b)]. Apart from masking out non-forest areas, it also removed some of the healthy identified trees [Figure 3.4 (a)]. It was further clarified by Figure 3.2 (b) where the trees were visible. The total number of trees that were masked out in the process can be referred from Table 3.3. Broadleaved trees were mostly seen removed in the process compared to the needle leaved tree species (Table 3.3).

Similarly, ITC Valley Following process produced bitmap [Figure 3.2 (c)]. It created valley of shade in between the tree crowns that can be seen in black colour. All the pixel value below the local minima which was set as 460 values formed valley of shade and separated potential tree crown. Some of the crowns were seemed to be under segmented.

Finally, the bitmap of distinct individual trees were obtained which is also referred to as "ISOLS". The ISOLS can be seen in Fig 2-5 (d) in green colour. In the crown isolation process some of the big crowns were broken into more than two crowns where as some of the overlapped tree crowns could not be separated. It was also noticed that some of the broadleaved tree crowns were delineated small. Thus the problem of over-segmentation and under-segmentation persists in the segmentation.

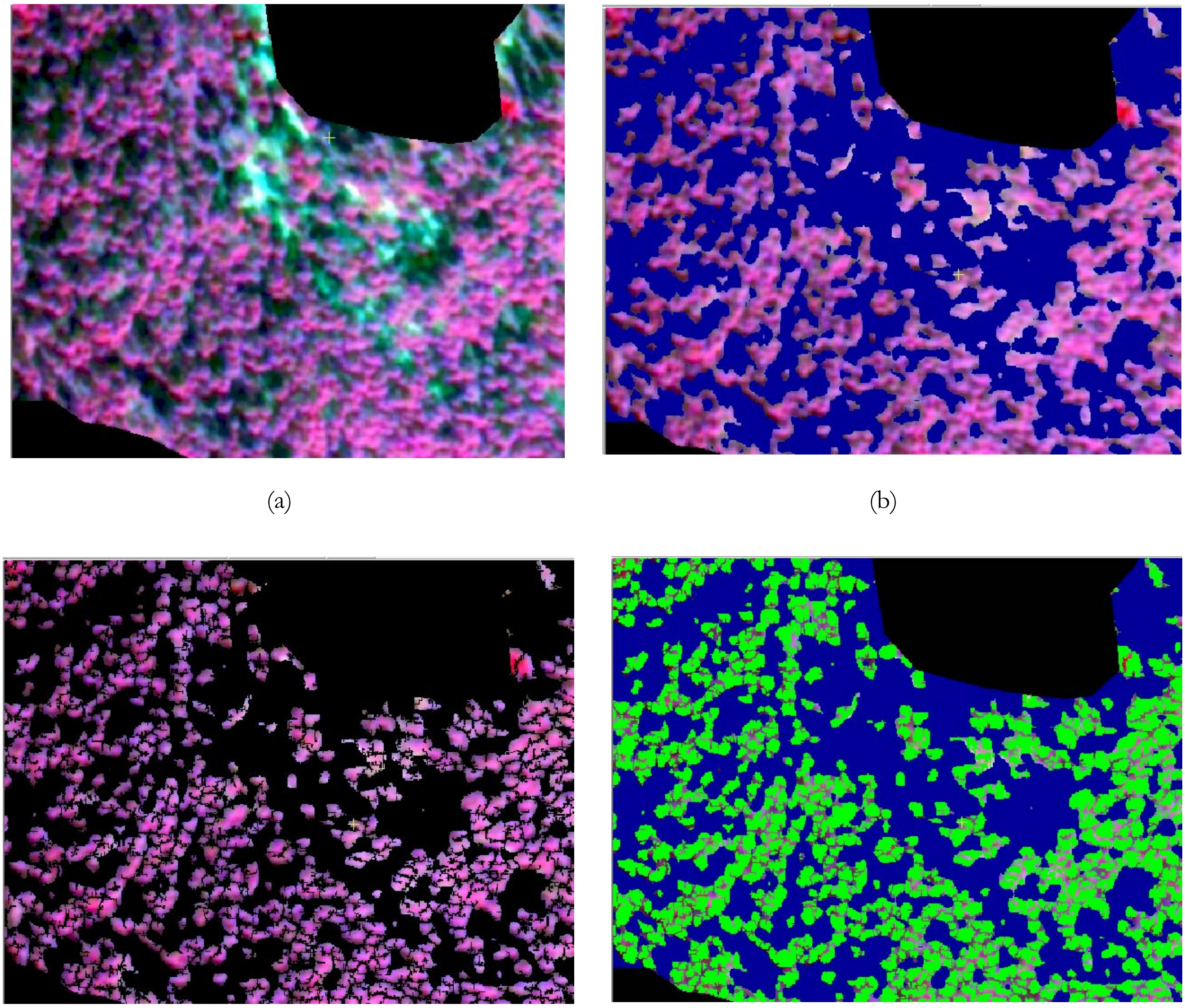

(a) (b)

(c) (d)

Figure 3.2 (a) Illustrated original image after filtering, (b) Mask out of non-forest area in blue colour, (c) The valley following shown in black colour and (d) The individual crown isolation in green colour

3.4. Segmentation Accuracy

The accuracy assessment of the 1:1 correspondence is presented in Table 3.3. The overall segmentation accuracy was found to be 60%. This implied that 60% of the CPA-segment had good match with the CPA-visual. Similarly, accuracy of the broadleaved and needle leaved tree species were found to be 66% and 56% respectively. This showed that 66% and 56% of the CPA-segment had good match with the CPA-visual. The missing tree were accounted as 12% out of which broadleaved were found missing by 81% and needle leaved by 19%. The missing tree was very high in broadleaved trees compared to needle leaved tree species. Figure 3.3 (a) showed the missing tree after the non-forested mask areas where as (b) clearly showed there were some trees which had gone missing.

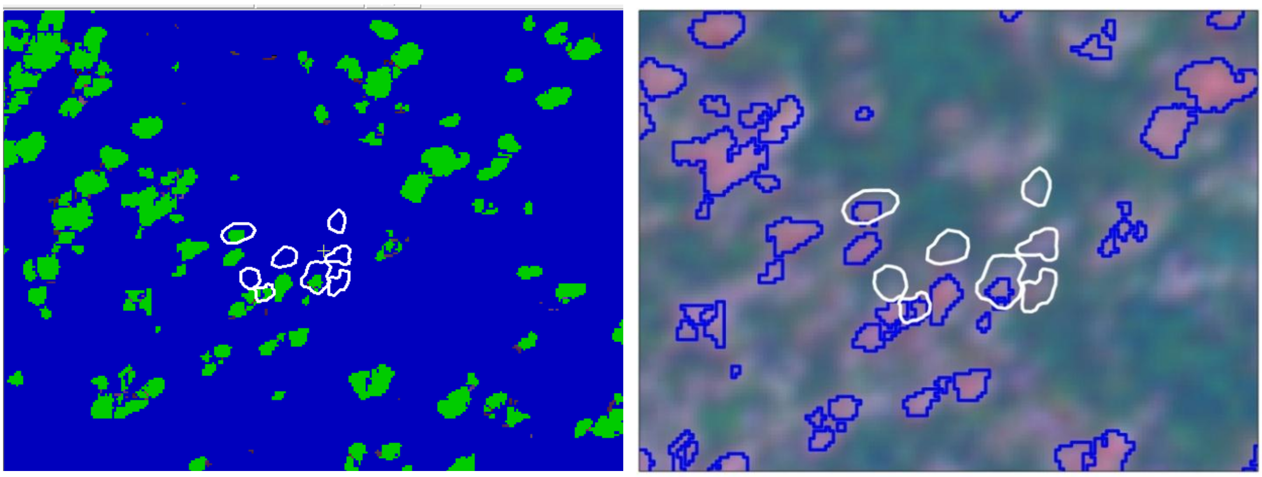

(a) (b)

Figure 3.3 Missing tree information (a) The missing tree from the illustrated area of bitmap (b) The enlarged missing tree information

The over-segmentation together with under-segmentation error or problem was found to be 27% irrespective of the broadleaved and needle leaved type. Figure 3.4 (b) showed that CPA-segments and CPA-visual are not matching and depicted some segmentation problem which can be clearly seen. The over-segmentation together with under-segmentation error revealed that 27% of the CPA-segments had less than 50% overlap with CPA-visual. After discarding the missing trees together with the over-segmented and under-segmented trees, the identified trees were reduced to 102 out of 170 trees (Table 3.3)

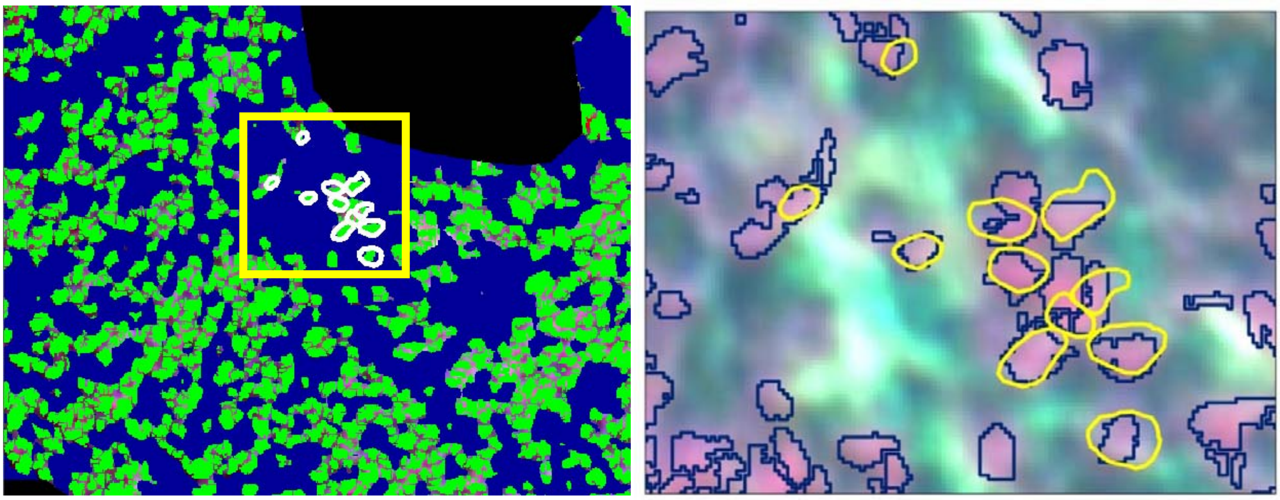

(a) (b)

Figure 3.4 Map showing visual comparison between CPA-Visual and CPA-Segments (a) CPA-Visual (in box) overlaid on CPA-Segments from bitmap of illustrated area (b) Enlarged box showing visual comparison between CPA-Visual in yellow and CPA-Segments in blue and over-segmentation and under-segmentation problem.

Table 3.3 The result of 1:1 correspondence

Type of Tree	Total trees No.	1:1 correspondence (≥50% crown overlap)		Missing trees		Segmentation problem	
		No.	Accuracy (%)	No.	Percentage	No.	Percentage
Needle leaf	71	47	66	4	19		
Broadleaved	99	55	56	17	81		
Total	**170**	**102**	**60**	**21**	**12**	**47**	**27**

3.5. Classification Accuracy

Spectral reflectance curve (Figure 3.5) of three major dominant trees (Pine, Alder and Schima) and one other group (group of few broadleaved trees) reflected high in NIR band followed by green and red band. Surprisingly, Pine trees were found to have high reflectance value followed by Alder trees. In general broadleaved trees have high reflectance value compared to needle leaved tree species. Although, Alder trees looked separable in NIR bank but while conserving the standard deviation, all the broadleaved trees were not separable (Table 3.4)Table 3.4 The pixel value of the species across NIR, Red and Green band. Thus the trees were more separable when all broadleaved trees were grouped in broadleaved trees.

Table 3.4 The pixel value of the species across NIR, Red and Green band

Band	Pinus		Alnus		Schima		Others	
	Std. dev	Mean	Std. dev	Mean	Std. dev	Mean	Std. dev	Mean
NIR	65.19	771.36	109.76	712.04	60.05	660.83	78.35	658.20
Red	39.53	385.23	25.10	351.98	21.11	330.67	17.92	339.96
Green	60.00	657.54	42.26	573.69	37.45	566.73	24.28	571.89

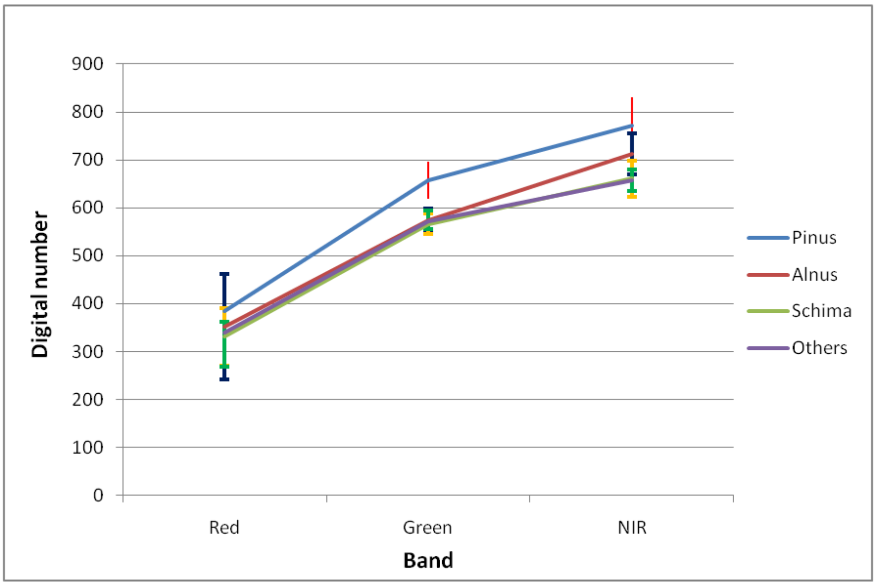

Figure 3.5 Spectral reflectance of the species in red, green and NIR band

The classification accuracy of broadleaved tree for three classes is presented in the (Table 3.5). Overall classification accuracy and Kappa coefficient for three classes was found to be 63% and 0.40 respectively. This meant that 63% of the CPA-segments were correctly classified. The accuracy assessment showed that classification for needle leaved Pine tree was high with the user's accuracy of 96%. Similarly, user's accuracy for the broadleaved Alder trees and others was found to be 58% and 13.33% respectively. This showed that classification for other broadleaved tree was low. However, Landis and Koch (1977) defined the agreement criteria for Kappa statistic as poor when K<0.4, good when 0.4<K<0.7 and excellent when K>0.75.

Table 3.5 Error matrix of three classes

Classified Data	**Pine**	**Alnus**	**Others**	**Reference Totals**	**Row Total**	**Number Correct**	**Producer Accuracy**	**Users Accuracy**
Pine	24	1	0	31	25	24	77.42%	96.00%
Alnus	1	7	4	15	12	7	46.67%	58.33%
Others	6	7	2	6	15	2	33.33%	13.33%
Total	**31**	**15**	**6**	**52**	**52**	**33**		
Over all accuracy = 63.46								
Kappa coefficient = 0.4								

The 63% accurate classified map of three classes is shown in the Figure 3.6. The small box showed the classified map of the illustrated area.

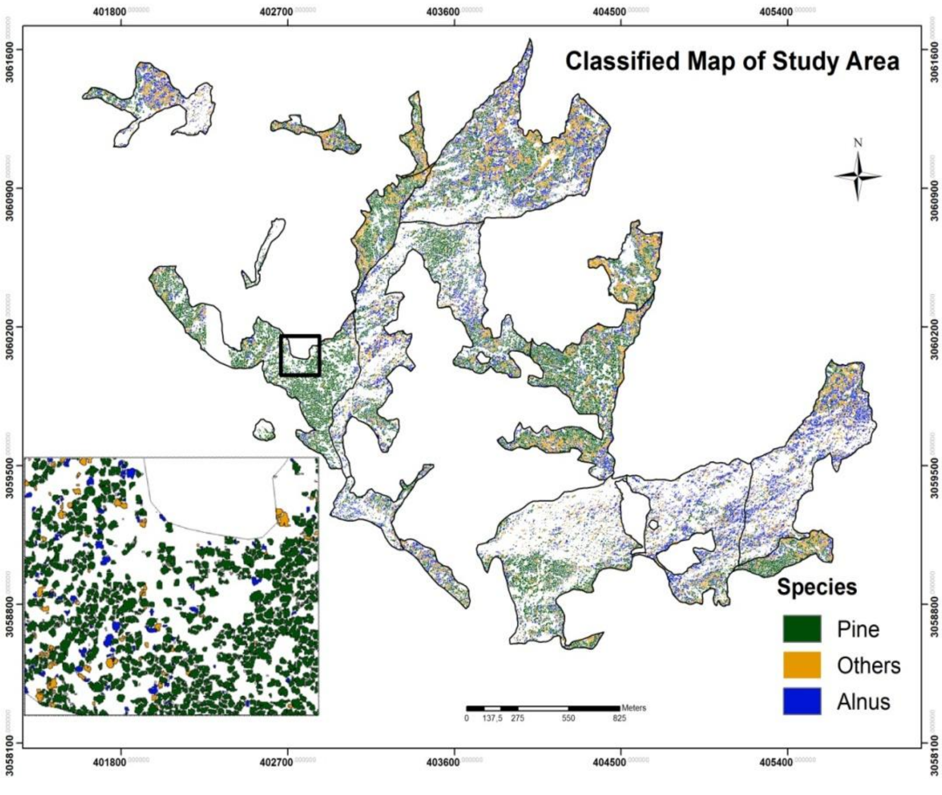

Figure 3.6 The classified map of 3 classes and box shows the classified map of the illustrated area

Similarly, the accuracy assessment of classification in two classes of broadleaved and needle leaved tree species is presented in the Table 3.4. When the broadleaved were grouped it resulted in 81% classification accuracy and Kappa coefficient was 0.63 respectively. The accuracy assessment showed that 81% of the both broadleaved and needle leaved was correctly classified. It was found that user accuracy of needle leaved Pine was very high which reached 100%. Similarly, user's accuracy for the broadleaved trees was found to be 67% (Table 3.6).

Table 3.6 Error matrix of broadleaved and needle leaved trees

Classified Data	Broadleaved	Needle leaved	Reference Totals	Row Total	Number Correct	Producer Accuracy	Users Accuracy
Needle leaved	0	21	31	21	21	67.74%	100.00%
Broadleaved	21	10	21	31	21	100.00%	67.74%
Total	**21**	**31**	**52**	**52**	**42**		
Over all accuracy = 80.77%							
Kappa coefficient = 0.63							

The 81% accurate classified map in two classes is shown in the Figure 3.7 with the illustrated area in the small box.

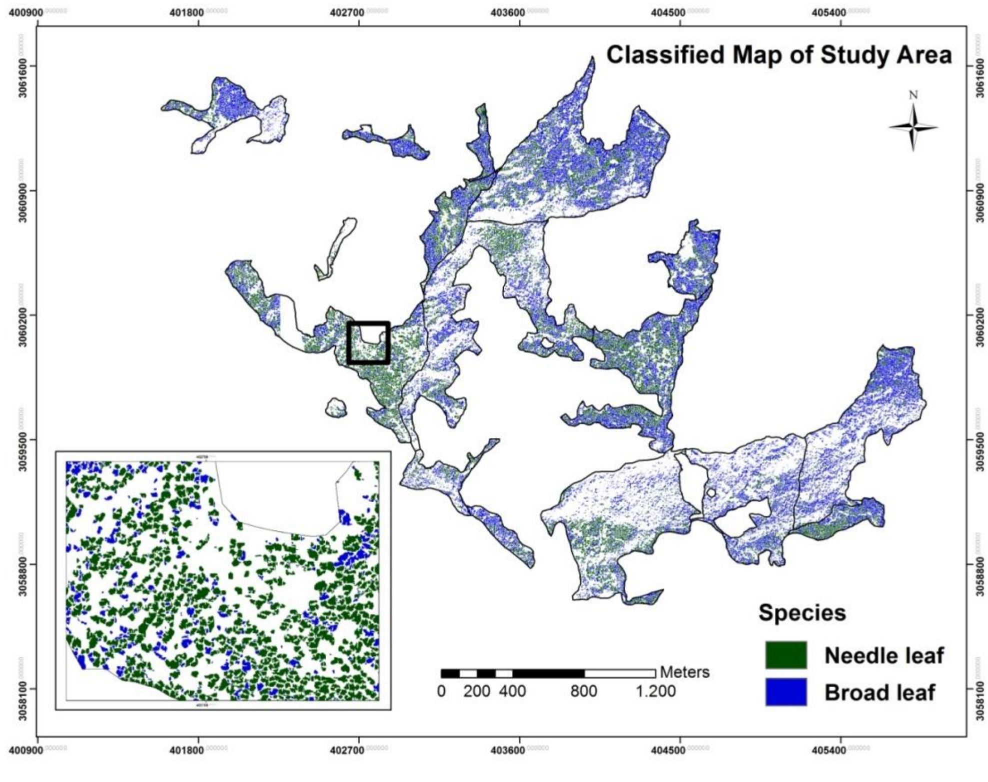

Figure 3.7 The classified map of two classes and small box showed classified map of illustrated area

3.6. DBH-CPA relationship for broadleaved and needle leaved tree species

The correlation between DBH against CPA segmented for broadleaved trees was found to be positive but the relationship between them was weak. The correlation coefficient (R) and coefficient of determinants (R^2) was found as 0.35 and 0.12 respectively. The result showed that there was almost no relationship between DBH-CPA segmented. Similarly, R and R^2 for the CPA-Carbon were found to be 0.61 and 0.38 respectively. The R and R^2 were slightly higher than DBH-CPA segmented relationship but still the relationship between them was weak. Figure 3.8 (a) showed that DBH against CPA-segmented points were very much scattered away from the regression line.

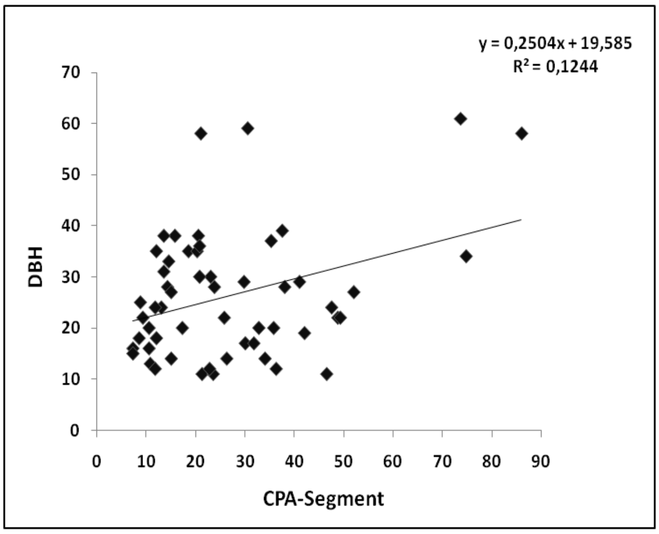

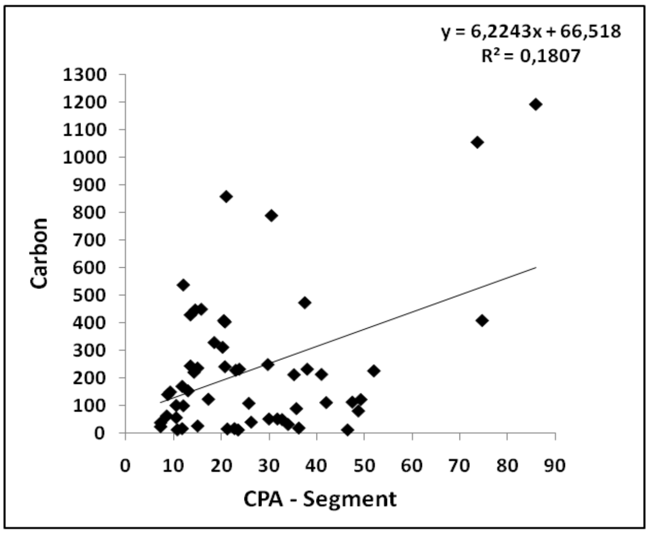

(a) (b)

Figure 3.8 CPA/Carbon and DBH relationship for broadleaved trees (a) CPA and DBH (b) CPA and Carbon

Similarly, the correlation between DBH and CPA segmented for needle leaved tree species was found to be positive with R 0.59 and the relationship was found to be weak with R^2 of 0.35. Similarly, R and R^2 for the CPA-Carbon was 0.61 and 0.38 respectively.

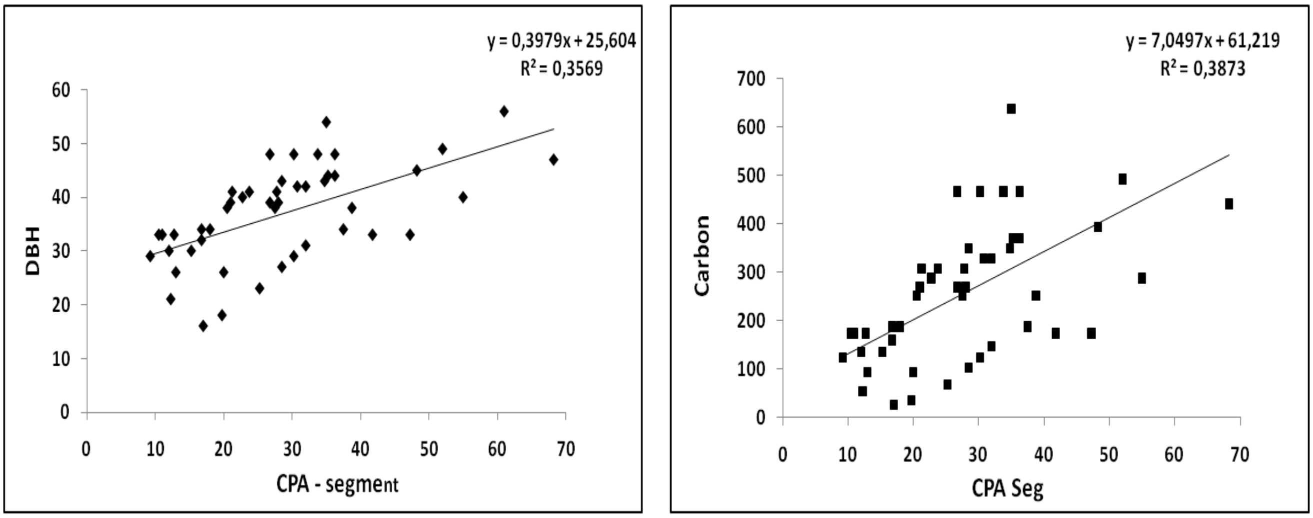

(a) (b)

Figure 3.9 CPA/Carbon and DBH relationship for needle leaved tree species (a) CPA and DBH (b) CPA and Carbon

3.7. Model development and validation

3.7.1. Modelling of broadleaved trees

The result of the linear regression and Root Mean Square Error (RMSE) for broadleaved tree species for 38 training data is presented in Table 3.7 and Table 3.8 . The model was significant as Pr>F (Table 3.8). Similarly, the R^2 was found to be 0.06 which was very low. Similarly, RMSE for validation, with 17 validating data (n=17), was found to be 230.41 kg (*i.e.* RMSE% was 84%). The result of RMSE for broadleaved showed that model had error of 84% which was very high. The hypothesis was failed to reject since R^2 was very low and RMSE% was not equal to or less than 30%. This meant that carbon prediction model could not be considered as good model as it can predict only 16% carbon with respect to the measured carbon in the field. (See details in Table 3.7). The carbon prediction model equation (4) is shown below:

$$\text{Carbon} = 118.46 + 6.67 * \text{CPA Seg} \qquad (4)$$

Where,
Intercept (a) = 118.46
Slope (b) = 6.67

Table 3.7 Summary of the model for broadleaved trees

Trees	R^2	**N**	**RMSE (kg.) (Validation n=17))**	**RMSE %**	**Equation**
Broadleaf	0.06	38	230.41	83.50	Carbon = 118.46+6.67*CPA Seg

Table 3.8 Analysis of variance for broadleaved trees

Source	DF	Sum of squares	Mean squares	F	Pr > F
Model	1	533150,61	533150,61	2,640	0,113
Error	37	7471961,13	201944,89		
Corrected Total	38	8005111,74			

3.7.2. Modelling of needle leaved tree species

The result of the linear regression and Root Mean Square Error (RMSE) for needle leaved tree species carried out with 32 training data is presented in Table 3.9 and Table 3.10. The R^2 with 0.39 was not good. Similarly, RMSE for validation, with 15 validating data (n=15), was found to be 120 kg (*i.e.* RMSE% was 45%). However, the model was significant as Pr>F (Table 3.10), the null hypothesis was failed to reject since R^2 was very low and the RMSE% was not equal to or less than 30%. This meant that carbon prediction model could not be considered as good model. It is because it can predict only 55% carbon with respect to the measured carbon in the field. (see details in Table 3.9). The carbon prediction model (equation 5) is shown below:

$$\text{Carbon} = 118.46+6.67*\text{CPA Seg} \qquad (5)$$

Where,
Intercept (a) = 118.46
Slope (b) = 6.67

Table 3.9 Summary of the model for needle leaved tree species

Trees	R^2	N	RMSE (kg) (Validation n = 15)	RMSE %	Equation
Pine	0.39	32	119.62	45.39	Carbon = 54.51+7.76*CPA Seg

Table 3.10 Analysis of variance for needle leaved tree species

Source	DF	Sum of squares	Mean squares	F	Pr > F
Model	1	312801,43	312801,43	22,578	< 0.0001
Error	31	429482,79	13854,28		
Corrected Total	32	742284,23			

3.8. Evaluation of the steps in processing

3.8.1. Verification of visual delineation

The RMSE for the visual delineation with respect to the field data was found to be 1.19m which is only 17%. Result showed crown diameter (CD) of the image explain 83% with respect to the measured field crown diameter. It revealed that the error is low and there was not much variance in the visual delineation of the tree crown. One to one relationship between measured CD of field and visual CD of image described that the points were very close to the diagonal except for few trees (Figure 3.10)

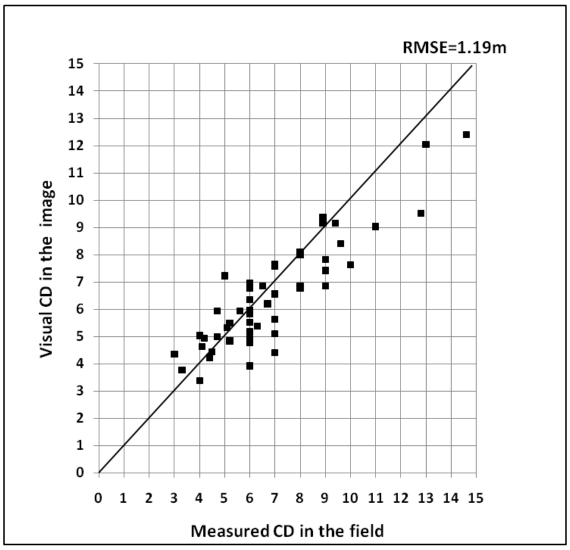

Figure 3.10 One to one matching of measured crown diameter in the field against visual crown diameter in the image

3.8.2. RMSE of segments of broadleaved and needle leaved

RMSE was found to be 70% and 45% for broadleaved trees and needle leaved tree species respectively. The RMSE of CPA-segmented in broadleaved was found very high compared to needle leaved tree species. This showed that CPA-segment of broadleaved and needle leaved trees can explain 55% and 30% with respect to the CPA-visual. The 1:1 relationship for needle leaved showed better result than broadleaved trees. (Figure 3.11).

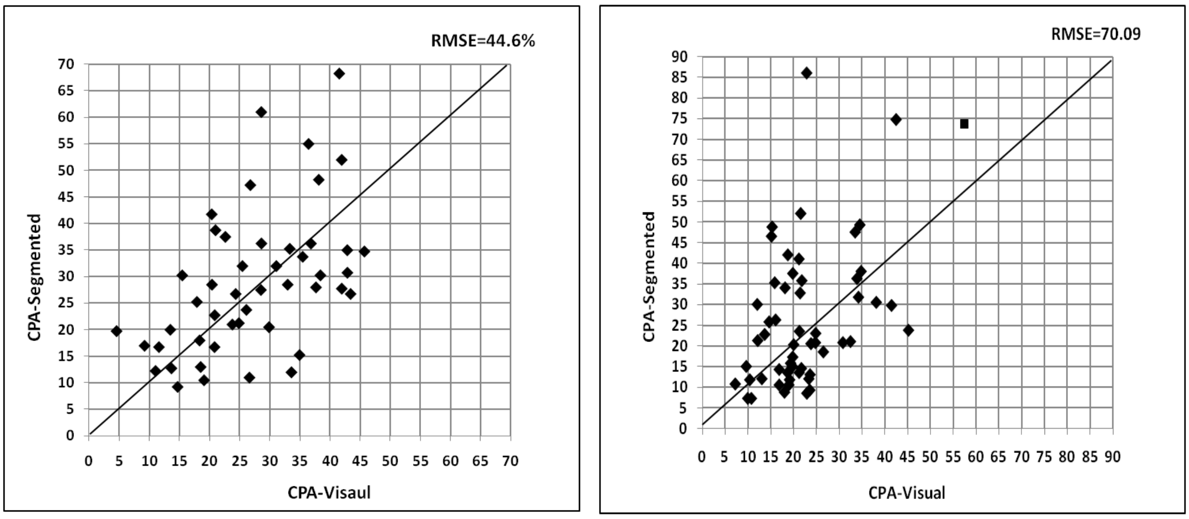

Figure 3.11 (a) RMSE for needle leaved tree species (b) RMSE for broadleaved tree species

3.8.3. CPA-visual and DBH- relationship for broadleaved and needle leaved tree species

The relationship between DBH and CPA visual for broadleaved tree species was found to be positive since R was 0.52. But the relationship was found to be weak since R^2 was 0.28 only [Figure 3.12 (a)].

Similarly, the relationship between DBH and CPA visual for needle leaved tree species was also found to be positive as R was 0.77. The relationship between them was found to be good sine R^2 was found to be 0.59. The scatter plot [Figure 3.12 (b)] showed that the points are scattered away from the regression line. The result showed good relationship for needle leaved Pine tree species.

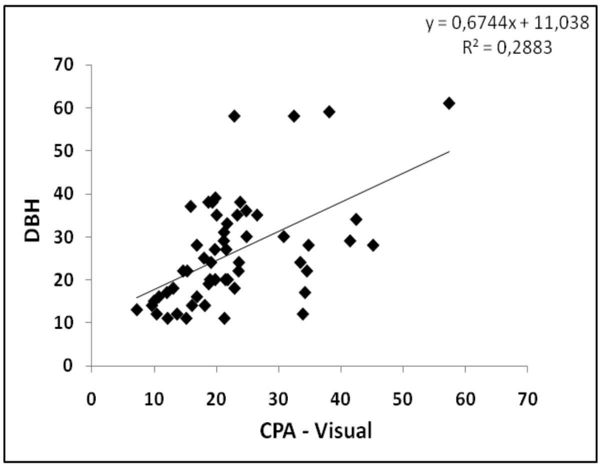

(a)

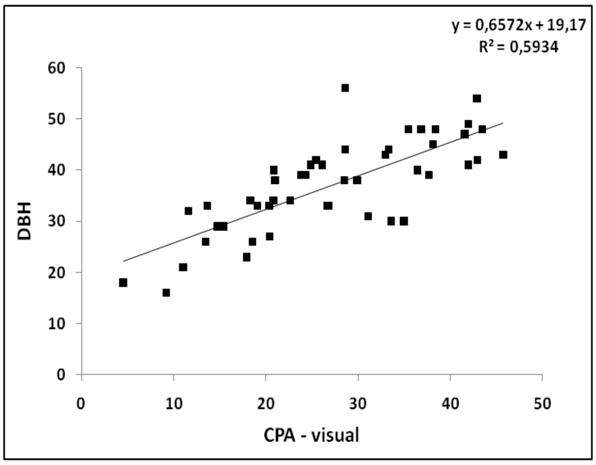

(b)

Figure 3.12 CPA visual and DBH relationship (a) broadleaved tree species (b) needle leaved tree species

4. DISCUSSION

The study was initiated expecting significant relationship of DBH and CPA for broadleaved and needle leaved tree species. It was also expected that significant relationship would provide carbon estimation model with high R^2 and low RMSE. The results related to the study are discussed in the separate sub headings.

4.1. Segmentation of the tree crown

The overall accuracy assessed in 1:1 correspondence was found to be 60% (Table 3.3). The accuracy for broadleaved and needle leaved tree species were found to be 66% and 56%. The missing trees were found to be 12% and it accounted more with broadleaved tree species with 17% compared to 6% of needle leaved tree species. Similarly the over-segmentation together with the under-segmentation was found to be 27%.

One of the reasons of lower accuracy was missing tree that started in the generation of forest mask as the process removed identified trees. Only the dead and unhealthy trees should have been removed (Gougeon, 2003) in the process. The removal of trees was initial problem in the masking out process (Ke, 2008; Leckie*, et al.*, 2005; Wang*, et al.*, 2004). The broadleaved Alder trees and *Schima wallichii* found in the shadowed region were mostly removed during the process. The removal of Alder trees were also due to the fact that they require moist surface which is available in the shadowed region (Barakoti, 2006). The chart (Figure 4.1) describes that broadleaved trees were mostly found on the northern and western aspect. These areas receive less sunlight throughout the day. These areas might have been in shadowed at the time (10.00 am) of image capture. Gougeon (2010b) in the suite manual also confirms that there might be some artefacts in the shadowed region.

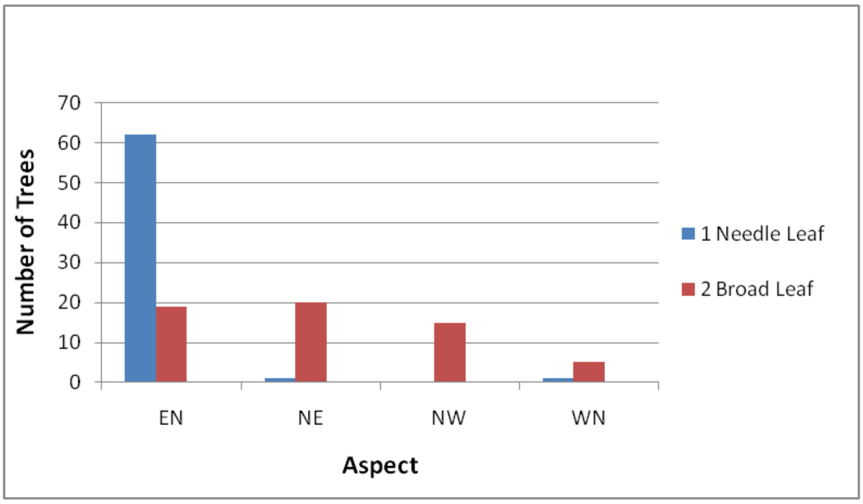

Figure 4.1 The distribution of tree aspect wise

After some trees were missed in the generation of forest mask, there were problem of over-segmentation and under-segmentation that appeared in the valley following process. Valley following process failed to create valleys in between the crown and also created valleys inside a single crown of a big tree. The lower threshold that was set to 460 failed to create valleys in between the tree crown because edges of the tree crowns were generally very bright. This affected in uniting multiple crowns into single tree crown. If this threshold was set a bit higher than edges of the crown were also removed. It is because value of the edges of standalone tree crown is always lower than overlapped tree. This affected in separating tree crown small. Despite these problem in lower threshold Gougeon (2003) implies that the selection of lower thresholds was not a big problem as it can also be done in automatic mode. The upper threshold that was set to 1015 did not limit the valley progression in high radiance (Gougeon, 2006) creating valleys within a single big tree. This problem was seen especially in broadleaved(Gougeon, 2006) *Schima wallichii* since they have big crown.

The problems in valley following affected in the crown isolation process. The crowns that were not separated well had problems of under segmentation and over segmentation and Gougeon (2010a) also admits that it is a problem that has to be minimized. It was observed that under segmentation was found to be prevalent in both needle leaved Pine trees as well as broadleaved Alder trees. Whereas over segmentation occurred mainly with the broadleaved *Schima wallichii.* It is because the branches in high resolution images are distinctly visible exhibiting the illumination variation within and between crowns. This illumination variation was caused by branches and shadow of the branches. Consequently, this characteristic of broadleaved species alters the spectral response of the crown (Zhengrong, *et al.*, 2008). Even a single tree might have huge branches which appear to resemble cluster of trees in the image consisting of a number of pixels with many different spectral values(Lamonaca*, et al.*, 2008). Further, individual tree crown delineation algorithms consider the tree tops to be conical in shape (Ke & Quackenbush, 2008) and considers the treetop to be the brightest point in the tree (Culvenor, 2002; Gonzalex, *et.al,* 201; Leckie, Donald G., *et.al.*,2005; Wang *et.al.,*2004)

ITC software can perform better when the sun elevation angle is as low possible and $\pm$ 15^0 from nadir (Gougeon, 2010b). The topography, off-nadir viewing and high sun elevation angle can alter the apparent tree size different from the real one (Song*, et al.*, 2010; Wulder*, et al.*, 2004). These issues can change the amount of shadows in the image although trees are always vertical regardless whether they grow. (Schaaf*, et al.*, 1994). Wulder *et. al.* (2004) explains the presence of shadows affects in obscuring some tree crowns in the image. The large view angle showed increasingly leaning trees as one got away from the image centre (nadir), making crown delineation difficult and increasing the probability of trees being completely hidden. (Gougeon, 2010a).

In addition, there was some distortion in the image that was found after the image was orthorectified. The distortion was found mainly on the steep slopes. Garrigus (2008) stated that low accuracy of DEM can lead to image distortion during orthorectification. But the accuracy 2m DEM cannot be responsible for this distortion. Although the study area was selected in the area devoid of distortion, the traces of distortion was seen at some places. The exact reason of the distortion could not be known.

Similar study was carried out by Leckie (2005) and obtained the segmentation accuracy of 59% adopting 1:1 correspondence. Although the accuracy was close to ours the study was also similar as it was carried out in natural mixed forest with canopy closure of 65 -85% except for gentle slope terrain. Similarly, Ke (2008) found segmentation accuracy 56% adopting 1:1 correspondence. The results of segmentation accuracy looked close to ours and the species was also mixed comprising both broadleaved and needle leaved. Another study carried out by Wang *et.al* (2004)found the segmentation accuracy of 75%. This segmentation accuracy looked very high compared to ours. The accuracy was found to be higher as the study area was flat with small area of 8 hectares only. In addition the study area had sufficient gap in between the trees (Wang, *et.al.* 2004).

4.2. Species Classification

The reflectance curve showed that Pine trees had higher reflectance value followed by Alder trees. In general reflectance value of broadleaved trees is higher than needle leaved Pine trees (Katoh*, et al.*, 2009). It was because needle leaved tree species are light demander and grow on east and south facing slopes (Figure 4.1). While most of the broadleaved trees are found to be grown on the north and west facing slope. The time of image acquisition and the season also affects the spectral reflectance. The image was captured at 10.00 am (local time) indicating needle leaved tree species receiving enough sunlight compared to very little sunlight in north and west facing slopes. In addition, the leaves of broadleaved trees tend to change the colour in the late autumn season resulting in poor separability among the broadleaved trees.

Accuracy assessment for the classification of three classes was found to be 63% with the Kappa statistics of 0.4. It was also observed that user accuracy was very high for the needle leaved Pine tree species. It was moderate with Alder tree species and poor with other broadleaved trees. The poor classification result with the broadleaved tree species was due to the close reflectance value. Some of the broadleaved trees growing on the eastern aspect can show their high reflectance and could be classified as needle leaved trees (Katoh*, et al.*, 2009).

The accuracy assessment in two classes as broadleaved and needle leaved tree species was found to be 81% with Kappa coefficient of 0.6. The user accuracy of needle leaved Pine trees was still higher compared to broadleaved trees. Although, good crown isolation can lead to good species classification, over-segmentation and under-segmentation problem hardly matters during classification. It is because over-segmentation does not give big problem as it could be recovered during the classification of the ISOLS (Janssen & Molenaar, 1995). Usually, with the increase in number of ISOLS, errors are expected to decrease (Biswas & Pal, 2000). Conversely, under-segmentation affects the species classification as it cannot be recognized during classification and it result in mis-identification of the crown (Carleer*, et al.*, 2005).

The study carried out by Erikson (2004) obtained 91% classification accuracy for the broadleaved and needle leaved tree species. The accuracy was higher compared to our result and it is similar to our case that it is a natural mixed forest. It is different in our case that they used airborne sensor and adopted Brownian motion for segmentation and the terrain is not that hilly compared to ours.

4.3. DBH-CPA relationship and linear regression model

The relationships of DBH and CPA-segment in the study area were not good as the goodness of fit (R^2) was 0.35 and 0.12 for needle leaved and broadleaved trees respectively. Infact, the relationship was found poor and almost no relationship for the broadleaved tree species compared to the needle leaved tree species. The reason for not obtaining good DBH and CPA-segment relationship is mainly the low segmentation accuracy. There was over-segmentation and under-segmentation problem. Thus, the high errors in CPA extraction passed on to the low DBH and CPA-segmented relationship.

Similarly, linear regression model was developed for broadleaved and needle leaved tree species due to the fact that most of the trees in the study area were considered as young since the mean DBH for broadleaved tree was 19cm and mean DBH for needle leaved tree was 26cm (Table 3.1 and Table 3.2). Since, the trees having 10cm DBH were not measured the mean DBH could even go below than mentioned above or as in Table 3.1 and Table 3.2. In the young age DBH and crown increases linearly and later crown increase in decreasing rate after the canopy starts touching each other (Shimano, 1997). The most of the broadleaved trees were considered young compared to needle leaved tree species. But due to natural forest type their canopy were touching each other. The RMSE% from the validation showed that carbon predicting model for broadleaved can estimate only 16% with respect to the measured carbon in the field. Similarly, the carbon predicting model for needle leaved tree species can predict up to 55% with respect to the measured carbon. Both of the models could not be considered good model due to low R^2 and high error. The insignificant model for the broad leaved trees was mainly due to the poor segmentation which occurred mostly with the broadleaf compared to needle leaved.

The outcome of the DBH-CPA relationships in the study area was found to be very poor compared to the study of Shimano (1997) where he found R^2 as 0.90 and 0.86 for deciduous and conifers respectively. The study of Shimano (1997) was different from ours in three ways. Firstly, he measured both DBH and CPA from the field. Secondly, he carried out his study in sample cohorts with light competition between the trees. Thirdly, his study area was very small and there was no effect of topography. In our case DBH was measured in the field and CPA-segments were extracted from the image using ITC software. Similarly our study area was very large and trees were found in overlapped situation competing with each other. In addition, the topography of high mountains created shadows, and average slope ranged from 25^0 - 70^0 (Appendix 1).

4.4. Evaluation of the steps processing

The Figure 4.2 describes the steps of evaluation in the process of segmentation. The first step of the evaluation in the process was to verify the visual delineation. The result showed that there was error of 1m (*i.e.* only 17%). It indicated that there is no much variance in visual delineation and our validation data is good. It can be also considered good as crown diameter often measured in the interval of 0.5 m. Sometime crown diameter could be underestimated due to limited visibility due to overlapping (Grote, 2003).

The next step was to evaluate the process in the segmentation. Although, overall accuracy assessment obtained from 1:1 correspondence was found to be 60%. The RMSE was found to be 70% and 45% for the broadleaved and needle leaved tree species. It envisaged that there is high error in the broadleaved trees compared to the needle leaved trees. With this, it can be concluded that segmentation of broadleaved can only explain 30% with respect to the reference CPA-visual. With this high error the estimation of carbon can not be accurate (Gougeon, 2010a).

The third step was carried out to evaluate the CPA-visual and DBH relationship. The result showed that despite the low accuracy of the segmentation the relationship with the needle leaved trees was good. It revealed that there could be relationship if the segmentation could be improved. This evaluation highlighted that the main problem lie in segmentation and if segmentation could be improved the estimation of carbon stock could be assessed with higher accuracy.

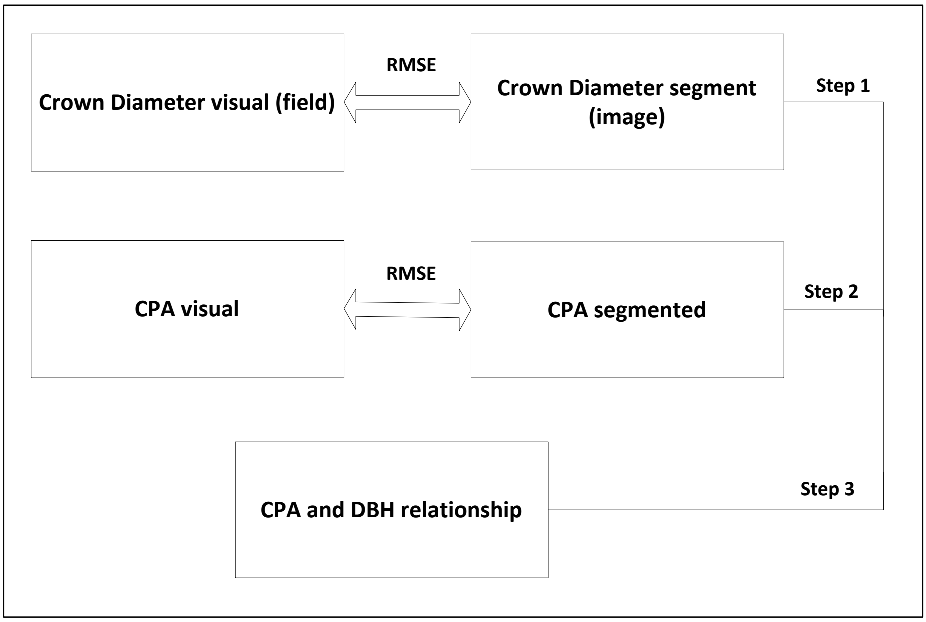

Figure 4.2 Steps of evaluation in the processing

4.5. Sources of error

Errors can be introduced at any steps from collection, processing and analysis of image and field data, and model development and finally propagated to the maps. (Wang, *et al.*, 2005). The Figure 4.3 describes mainly the three types of error that can be prevalent in the carbon estimation using high resolution image and object based image analysis. The first and foremost error is segmentation error which can be influenced by view angle, sun angle, topography and slope. The overlapping crown also cause to over-segmentation and under-segmentation.

The next error is the classification error, which when not accurate can not predict the carbon accurately. The source for classification error can be the sampling error, spectral characteristics of the vegetation, image geocoding and misidentification of the trees.

Further, the inappropriate selection of allometric equation and carbon predicting model further introduce the error. The use of wood density in the equation enhances the accuracy of the equation. This wood density is found to be different at various sections of a tree. It is usually higher at breast height compared to top of the stem (Nogueira, *et al.*, 2005). The measurement is also higher at the stump height compared to base of crown (Cordero, *et al.*, 2002). This emphasize that there can be error if only one measurement is taken for *e.g.* at DBH only (Basuki, *et al.*, 2009).

The selection of the allometric equation should be done very carefully as regression models should not be used beyond their range. It introduces some error if the diameter of the trees ranges from 15-50cm and the equation was used for more than 52cm. (Chave, *et al.*, 2005)

All these source of error accumulated and propagated giving inaccurate carbon estimation.

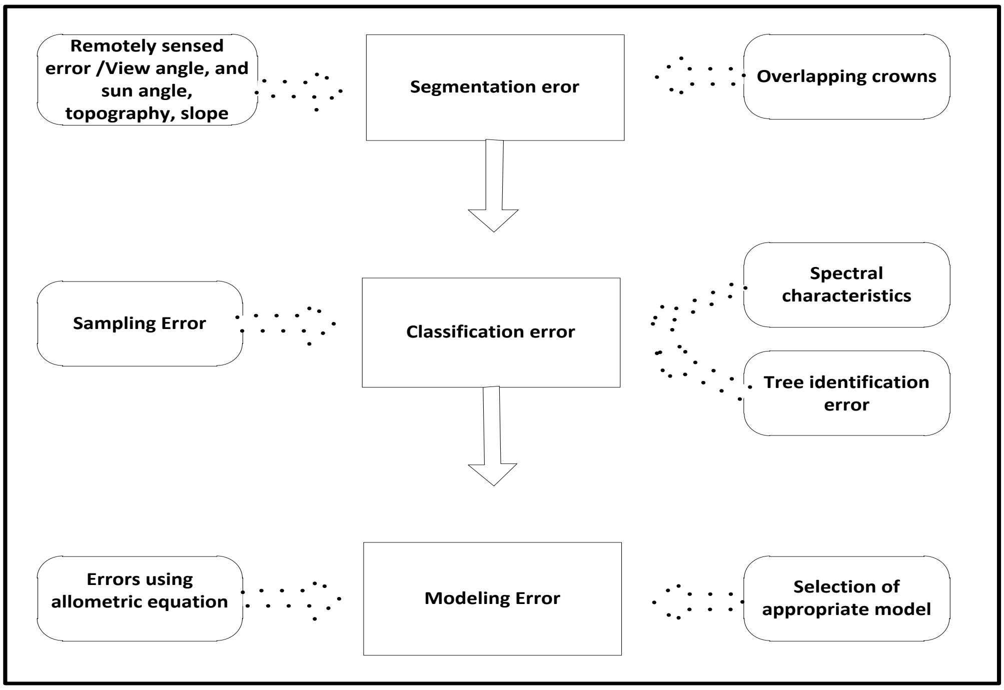

Figure 4.3 Sources of error [Adopted from (Wang, et al., 2005)]

5. CONCLUSION

A method was developed to estimate above ground carbon in high mountainous broadleaved and needle leaved forests using a very high resolution satellite imagery and individual tree crown segmentation (*i.e.*. object based image analysis). The following conclusions are made based on the specific objectives and the research questions as formulated in the introduction chapter.

Specific Objective 1: To identify the segmentation accuracy of the ITC software

What is the overall accuracy of segmentation using ITC software?
The overall accuracy of the segmentation using ITC software was assessed using 1:1 correspondence method. A moderate accuracy of 60% was found. It showed that 60% of the CPA-segments were matched as good (overlapping between the CPA-segments and CPA-visual ≥ 50%) with respect to the CPA-visual. Over segmentation together with under segmentation error was found to be 27%. It revealed that 27% of the CPA-segments were not good match (overlapping between the CPA-segments and CPA-visual < 50%) with respect to the CPA-visual.

What is the accuracy of segmentation in broadleaved trees and needle leaved tree species?
The segmentation worked differently in the oval or rounder shaped broadleaved tree crowns and the conical shaped pine tree crowns. It was found that the segmentation accuracy for pine (66%) was larger compared to broadleaved trees (55%).

Specific Objective 2: To identify the accuracy of species classification

Are the dominant trees in the study area separable from each other?
It was revealed from the spectral curve that all the trees have a high reflectance in the NIR followed by green and red bands. Pine trees were found to have highest reflectance values followed by Alder trees it is because they were found mostly on sunlit side while most of the others were found on shaded region. Schima and other broadleaved tree species could not be spectrally distinguished. Alder trees were separable with other broadleaved trees only in NIR band. But when considering the standard deviation of the reflectance Alder trees also could not be separated with other broadleaved trees. This showed that the species is well separated when grouped into broadleaved and needle leaved trees.

What is the overall classification accuracy of dominant trees?
The overall classification accuracy of the three dominant classes (*viz*. Pine, Alder and other broadleaved species) was 63 % and KAPPA was 0.4. The user accuracy for the pine was very high compared to alder and other broadleaved species. The accuracy increased to 81% from 63% in two classes when all the broadleaved were grouped into one class.

Specific Objective 3: To identify the relationship of DBH - CPA-segmented for broadleaved and needle leaved tree species

Is there any relationship between DBH and CPA-segmented and how strong is the relationship for both broadleaved and needle leaved tree species?

Positive relationships exist between field measured DBH and CPA derived from image segmentation (CPA-segmented) for both needle leaved and broadleaved trees. Although, the relationship was bit higher in needle leaved trees, both of the broadleaved and needle leaved trees had weak DBH and CPA-segmented relationship. The R^2 for broadleaved and needle leaved trees were 0.12 and 0.35 respectively.

Specific Objective 4: To develop the linear regression model to estimate above ground carbon for broadleaved and needle leaved tree species.

Does the linear regression model accurately estimate above ground carbon in broadleaved and needle leaved forest?

The linear regression model for the needle leaved trees was better compared to the broadleaved trees based on R^2 and RMSE. The R^2 for needle leaved and broadleaved trees were found to be 0.39 and 0.06 respectively. Similarly, RMSE was found to be 45% and 84% for needle leaved and broadleaved trees respectively. Both of these models could not be considered for carbon estimation since RMSE is more than 30%.

Specific Objective 5: To evaluate the processing steps in estimating carbon from very high resolution satellite image

What is the RMSE between visually delineated crown diameter and crown diameter of the tree measured in the field?

The RMSE was found to be 1.19m which is 17%. The visual crown diameter explained the crown diameter at higher (93%) accuracy.

What is the RMSE between CPA-segmented and CPA-visual?

RMSE for the broadleaved and needle leaved tree was found to be 70% and 45% respectively. The error was very high in broadleaved compared to the needle leaved tree species.

Is there any relationship between CPA-visual and DBH and how strong is the relationship for both broadleaved and needle leaved tree species?

There is a positive relationship between diameter at breast height (DBH) and crown projection area (CPA) for needle leaved Pine trees with R^2 of 0.59 implying that CPA-visual well represents differences in DBH. In the case of broadleaved trees the relation was weaker with an R^2 of 0.38

6. RECOMMENDATION

Above Ground Carbon estimation using very high resolution satellite imagery and individual tree crown delineation, segmentation, classification and modelling is a new approach. A lot many things were not known when the study was started. For instance the research design was made for 5996 ha. of forest and field data was collected accordingly. And all the pre-processing was done for the entire watershed. Then it had to be restricted to 297 ha. due to processing time required for software segmentation. Others issues are described below;

Season of data capture

The image was captured in late autumn season. The late autumn in the study area was the time where broadleaved trees tend to change colour of the leaves. It should be collected from summer time to early autumn.

Overlapping issue of tree crown

Overlapping issue of tree crowns persists in natural forest and it has to be studied as it has been one of the major problems for the software.

Integrating with LIDAR

Many studies showed that LIDAR gives accurate result. Integration of high resolution image with LIDAR would be highly recommended.

LIST OF REFERENCES

Andersson, K., Evans, T. P., & Richards, K. R. (2009). National forest carbon inventories: policy needs and assessment capacity. [Article]. *Climatic Change, 93*(1-2), pp 69-101.

Asner, G. P. (2009). Tropical forest carbon assessment: integrating satellite and airborne mapping approaches. *Environmental Research Letters, 4* (Copyright 2009, The Institution of Engineering and Technology), 11.

Asner, G. P., Palace, M., Keller, M., Pereira, R., Silva, J. N. M., & Zweede, J. C. (2002). Estimating canopy structure in an Amazon Forest from laser range finder and IKONOS satellite observations. *Biotropica, 34*(4), pp 483-492.

Asner, G. P., & Warner, A. S. (2003). Canopy shadow in IKONOS satellite observations of tropical forests and savannas. *Remote Sensing of Environment, 87*(4), pp 521-533.

Baatz, M., Benz, U., Dehghani, S., Heynen, M., Holtje, A., Hofmann, P., Lingenfelder, M., Sohlbach, M., Weber, M., Willhauck, G.,. (2004). *User Guide 4,* Definiens Imaging GmbH, Germany

Barakoti, T. P. (2006). Growth of Uttis (Alnus nepalensis) monitored in a trial plantation at Pakhribas, Dhankuta, Nepal. *Banko Janakari Vol 16, No 1*.

Basuki, T. M., van Laake, P. E., Skidmore, A. K., & Hussin, Y. A. (2009). Allometric equations for estimating the above-ground biomass in tropical lowland Dipterocarp forests. *Forest Ecology and Management, 257*(8), pp 1684-1694.

Bista, S., Shivakoti, G. (2000). Honeybee Flora at Kabre, Dolakha District. *Nepal Agriculture Research Journal, 4* pp *5*.

Biswas, S., & Pal, N. R. (2000). On hierarchical segmentation for image compression. *Pattern Recognition Letters, 21*(2), pp 131-144.

Bottcher, H., Eisbrenner, K., Fritz, S., Kindermann, G., Kraxner, F., McCallum, I., & Obersteiner, M. (2009). An assessment of monitoring requirements and costs of 'Reduced Emissions from Deforestation and Degradation'. *Carbon Balance and Management, 4*(1), pp 7.

Böttcher, H., Freibauer, A., Obersteiner, M., & Schulze, E.-D. (2008). Uncertainty analysis of climate change mitigation options in the forestry sector using a generic carbon budget model. *Ecological Modelling, 213*(1), pp 45-62.

Brack, C. L. (2004). Mensuration | Timber and Tree Measurements. In B. Jeffery (Ed.), *Encyclopedia of Forest Sciences* (pp. 566-573). Oxford: Elsevier.

Brandtberg, T., Warner, T. A., Landenberger, R. E., & McGraw, J. B. (2003). Detection and analysis of individual leaf-off tree crowns in small footprint, high sampling density lidar data from the eastern deciduous forest in North America. *Remote Sensing of Environment, 85*(3), pp 290-303.

Brown, S. (1997). *Estimating Biomass and Biomass Change of Tropical Forests: a Primer. (FAO Forestry Paper - 134).* Rome, FAO

Brown, S. (2002). Measuring carbon in forests: current status and future challenges. *Environmental Pollution, 116*(3), pp 363-372.

Brown, S., & Lugo, A. E. (1992). Above Ground Biomass estimates for tropical moist forests of the Brazilian Amazon. *Interciencia, 17*(1), pp 8-18.

Carleer, A. P., Debeir, O., & Wolff, E. (2005). Assessment of very high spatial resolution satellite image segmentations. *Photogrammetric Engineering and Remote Sensing, 71*(11), pp 1285-1294.

Chaturvedi, O., P., Singh, J., S.,. (1982). Total biomass and biomass production of Pinus roxburghii trees growing in all-aged natural forests. *Canadian Journal for Forest Resources, 12*, pp 632-640.

Chave, J., Andalo, C., Brown, S., Cairns, M. A., Chambers, J. Q., Eamus, D., Folster, H., Fromard, F., Higuchi, N., Kira, T., Lescure, J. P., Nelson, B. W., Ogawa, H., Puig, H., Riera, B., & Yamakura, T. (2005). Tree allometry and improved estimation of carbon stocks and balance in tropical forests. *Oecologia, 145*(1), pp 87-99.

Clinton, N., Holt, A., Scarborough, J., Yan, L., & Gong, P. (2010). Accuracy Assessment Measures for Object-based Image Segmentation Goodness. *Photogrammetric Engineering and Remote Sensing, 76*(3), pp 289-299.

Cochran, & Dalenius. (2006). Sampling in Forest Surveys. In M. KÖHL, S. MAGNUSSEN & M. MARCHETTI (Eds.), *Sampling Methods, Remote Sensing and GIS Multiresource Forest Inventory* (pp. 106). New York: Springer-Verlag Berlin Heidelberg.

Cohen, W. B., & Justice, C. O. (1999). Validating MODIS Terrestrial Ecology Products: Linking In Situ and Satellite Measurements. *Remote Sensing of Environment, 70*(1), pp 1-3.

Cordero, P., Diego, L., & Markku, K. (2002). Wood specific gravity and aboveground biomass of Bombacopsis quinata plantations in Costa Rica. *Forest Ecology and Management, 165*(1-3), pp 1-9.

Culvenor, D. S. (2002). TIDA: an algorithm for the delineation of tree crowns in high spatial resolution remotely sensed imagery. *Computers & Geosciences, 28*(1), pp 33-44.

DDC/LGP. (1999). *District Situational Analysis of Dolkha (District Profile)*, Dolakha, Nepal

Dixon, R. K., Brown, S., Houghton, R. A., Solomon, A. M., Tresier, M.C., Wisniewski. (1994). Carbon Pools and Flux of global forest Ecosystems. *Science (Washington DC), pp 263.*

Erikson, M. (2004). Species classification of individually segmented tree crowns in high-resolution aerial images using radiometric and morphologic image measures. *Remote Sensing of Environment, 91*(3-4), pp 469-477.

Fisher, P. (1997). The pixel: A snare and a delusion. [Proceedings Paper]. *International Journal of Remote Sensing, 18*(3), pp 679-685.

Fuchs, H., Magdon, P., Kleinn, C., & Flessa, H. (2009). Estimating aboveground carbon in a catchment of the Siberian forest tundra: Combining satellite imagery and field inventory. *Remote Sensing of Environment, 113*(3), pp 518-531.

Garrigus, A., Gleitsmann, A., . (2008). *Collecting and Processing Hi Resolution Satellite Imagery in Rural Areas of Alaska.*

GeoEye. (2011). GeoEye: The World's Highest-Resolution Commercial Satellite. Retrieved 7 Feb 2011, from http://www.geoeye.com/CorpSite/products-and-services/Default.aspx

Gibbs, H. K., Brown, S., Niles, J. O., & Foley, J. A. (2007). Monitoring and estimating tropical forest carbon stocks: Making REDD a reality.

Gonzalez, P., Asner, G. P., Battles, J. J., Lefsky, M. A., Waring, K. M., & Palace, M. (2010). Forest carbon densities and uncertainties from Lidar, QuickBird, and field measurements in California. *Remote Sensing of Environment, 114*(7), pp 1561-1575.

Gougeon, F. A. (2010a). Forest Remote Sensing in Canada and the Individual Tree Crown (ITC) Approach to Forest Inventories. *Journal of the Faculty of Agriculture SHINSHU UNIVERSITY, VOL.46 No. 1*2.*

Gougeon, F. A. (2010b). *The ITC Suite Manual, A Semi-Automatic Individual Tree Crown (ITC) Approach to Forest Inventories*. Victoria, British Columbia, Canada.

Gougeon, F. A., & Leckie, D. (2003). *Forest information extraction from high spatial resolution images using an individual tree crown approach* (No. BC-X-396), Victoria, British Columbia, Canada.

Gougeon, F. A., Leckie, D. G. (2006). The individual tree crown approach applied to Ikonos images of a coniferous plantation area. [Article]. *Photogrammetric Engineering and Remote Sensing, 72*(11), pp 1287-1297.

Grainger, A., Boucher, D. H., Frumhoff, P. C., Laurance, W. F., Lovejoy, T., McNeely, J., Niekisch, M., Raven, P., Sodhi, N. S., Venter, O., & Pimm, S. L. (2009). Biodiversity and REDD at Copenhagen. *Current Biology, 19*(21), pp 974-976.

Grote, R. (2003). Estimation of crown radii and crown projection area from stem size and tree position. *Ann. For. Sci., 60*(5), pp 393-402.

Gschwantner, T., Schadauer, K., Vidal, C., Lanz, A., Tomppo, E., di Cosmo, L., Robert, N., Duursma, D., & Lawrence, M. (2009). Common tree definitions for national forest inventories in Europe. *Silva Fennica, 43*(2), pp 303-321.

Hay, G. J., Castilla, G., Wulder, M. A., & Ruiz, J. R. (2005). An automated object-based approach for the multiscale image segmentation of forest scenes. *International Journal of Applied Earth Observation and Geoinformation, 7*(4), pp 339-359.

Hemery, G. E., Savill, P. S., & Pryor, S. N. (2005). Applications of the crown diameter-stem diameter relationship for different species of broadleaved trees. *Forest Ecology and Management, 215*(1-3), pp 285-294.

Hese, S., Lucht, W., Schmullius, C., Barnsley, M., Dubayah, R., Knorr, D., Neumann, K., Riedel, T., & Schröter, K. (2005). Global biomass mapping for an improved understanding of the CO2 balance--the Earth observation mission Carbon-3D. *Remote Sensing of Environment, 94*(1), pp 94-104.

Husch, B., Beers, T. W., & Kershaw, J. A. (2003). *Forest mensuration* (Fourth edition ed.). Hoboken: Wiley & Sons.

ICIMOD. (2010). *Report on forest carbon stocks in Ludikhola, Kayarkhola and Charnawati Watersheds of Nepal.* Kathmandu.

IPCC. (2003). Good Practice Guidance for Land Use, Land-Use Change and Forestry.

Janssen, L. F., & Molenaar, M. (1995). Terrain Objects, Their Dynamics and Their Monitoring by the Integration of GIS and Remote Sensing. *IEEE Transactions on Geoscience AND Remote Sensing,* vol. 33, NO. 3.

Kampouraki, M., Wood, G. A., & Brewer, T. R. (2008). Opportunities and limitations of object based image analysis for detecting urban impervious and vegetated surfaces using true-colour aerial photography. In T. Blaschke, S. Lang & G. J. Hay (Eds.), *Object-Based Image Analysis* (pp. 555-569): Springer Berlin Heidelberg.

Katoh, M., Gougeon, F., & Leckie, D. (2009). Application of high-resolution airborne data using individual tree crowns in Japanese conifer plantations. *Journal of Forest Research, 14*(1), pp 10-19.

Ke, Y., & Quackenbush, L. J. (2008). *Comparison of individual tree crown detection and delineation methods.* Paper presented at the American Society of Photogrammetry and Remote Sensing, Bethesda, Maryland, Portland, Oregon.

Krajicek, J. E., Brinkman, K. A., & Gingrich. S.F. (1961). Crown competition, a measure of density. *For. Sci, 7: pp 35-42.*

Lamonaca, A., Corona, P., & Barbati, A. (2008). Exploring forest structural complexity by multi-scale segmentation of VHR imagery. *Remote Sensing of Environment, 112*(6), pp 2839-2849.

Landis, J. R., & Koch, G. G. (1977). The Measurement of Observer Agreement for Categorical Data. *Biometrics, 33*(1), pp 159-174.

Leckie, D. G., Gougeon, F. A., Tims, S., Nelson, T., Burnett, C. N., & Paradine, D. (2005). Automated tree recognition in old growth conifer stands with high resolution digital imagery. *Remote Sensing of Environment, 94*(3), pp 311-326.

Leckie, D. G., Gougeon, F. A., Walsworth, N., & Paradine, D. (2003). Stand delineation and composition estimation using semi-automated individual tree crown analysis. *Remote Sensing of Environment, 85*(3), pp 355-369.

Lu, D. (2005). Aboveground biomass estimation using Landsat TM data in the Brazilian Amazon. *International Journal of Remote Sensing, 26*(12), pp 2509-2525.

Lu, D. (2006). The potential and challenge of remote sensing-based biomass estimation. *International Journal of Remote Sensing, 27*(7), pp 1297 - 1328.

Mallinis, G., Koutsias, N., Tsakiri-Strati, M., & Karteris, M. (2008). Object-based classification using Quickbird imagery for delineating forest vegetation polygons in a Mediterranean test site. *ISPRS Journal of Photogrammetry and Remote Sensing, 63*(2), pp 237-250.

Masera, O. R., Garza-Caligaris, J. F., Kanninen, M., Karjalainen, T., Liski, J., Nabuurs, G. J., Pussinen, A., de Jong, B. H. J., & Mohren, G. M. J. (2003). Modeling carbon sequestration in afforestation, agroforestry and forest management projects: the CO2FIX V.2 approach. *Ecological Modelling, 164*(2-3), pp 177-199.

Möller, M., Lymburner, L., & Volk, M. (2007). The comparison index: A tool for assessing the accuracy of image segmentation. *International Journal of Applied Earth Observation and Geoinformation, 9*(3), pp 311-321.

Nogueira, E. M., Nelson, B. W., & Fearnside, P. M. (2005). Wood density in dense forest in central Amazonia, Brazil. *Forest Ecology and Management, 208*(1-3), pp 261-286.

Patenaude, G., Hill, R. A., Milne, R., Gaveau, D. L. A., Briggs, B. B. J., & Dawson, T. P. (2004). Quantifying forest above ground carbon content using LiDAR remote sensing. *Remote Sensing of Environment, 93*(3), pp 368-380.

Rosenqvist, Å., Milne, A., Lucas, R., Imhoff, M., & Dobson, C. (2003). A review of remote sensing technology in support of the Kyoto Protocol. *Environmental Science & Policy, 6*(5), pp 441-455.

Santilli, M., Moutinho, P., Schwartzman, S., Nepstad, D., Curran, L., & Nobre, C. (2005). Tropical Deforestation and the Kyoto Protocol. *Climatic Change, 71*(3), pp 267-276.

Schaaf, C. B., Li, X. W., & Strahler, A. H. (1994). Topographic effects on bidirectional and hemispherical reflectances calculated with a geometric-optical canopy model *IEEE Transactions on Geoscience and Remote Sensing, 32*(6), pp 1186-1193.

Shimano, K. (1997). Analysis of the relationship between DBH and crown projection area using a new model. *Journal of Forest Research, 2*(4), pp 237-242.

Shinozaki, K., Yoda, K., Hozumi, K., & Kira, T. (1964). A Quantitative Analysis of Plant Form -- The Pipe Model Theory I. Basic Analyses. *Japanese Journal of Ecology, 14*(3), pp 97-105.

Smith, W. R., Farrar, R. M., Murphy, P. A., Yeiser, J. L., Meldahl, R. S., & Kush, J. S. (1992). Crown and basal area relationships of open-grown southern Pines for modeling competition and growth *Canadian Journal of Forest Research-Revue Canadienne De Recherche Forestiere, 22*(3), pp 341-347.

Song, C., Dickinson, M. B., Su, L., Zhang, S., & Yaussey, D. (2010). Estimating average tree crown size using spatial information from Ikonos and QuickBird images: Across-sensor and across-site comparisons. *Remote Sensing of Environment, 114*(5), pp 1099-1107.

Thomas, N., Hendrix. C., Congalton. R.G. (2003). A Comparison of Urban Mapping Methods Using High-Resolution Digital Imagery. *American Society for Photogrammetry and Remote Sensing Environment. 69*(9), pp 963-972.

Verplanke, J. J., & Zahabu, E. (2009). *field guide for assessing and monitoring reduced forest degradation and carbon sequestration by local communities : research project Kyoto : think global, act local*. Enschede: ITC.

Wang, G. X., Gertner, G. Z., Fang, S. F., & Anderson, A. B. (2005). A methodology for spatial uncertainty analysis of remote sensing and GIS products. *Photogrammetric Engineering and Remote Sensing, 71*(12), pp 1423-1432.

Wang, L., Gong, P., & Biging, G. S. (2004). Individual tree-crown delineation and treetop detection high-spatial-resolution aerial imagery. *Photogrammetric Engineering and Remote Sensing, 70*(3), pp 351-357.

Wulder, M. A., White, J. C., Niemann, K. O., & Nelson, T. (2004). Comparison of airborne and satellite high spatial resolution data for the identification of individual trees with local maxima filtering. *International Journal of Remote Sensing, 25*(11), pp 2225 - 2232.

Yang, L., Albregtsen, F., Lonnestad, T., & Grottum, P. (1995). *A supervised approach to the evaluation of image segmentation methods*. Paper presented at the Proceedings of 6th International Conference on Computer Analysis of Images and Patterns, 6-8 Sept. 1995, Berlin, Germany.

Zhan, Q., Molenaar, M., Tempfli, K., & Shi, W. (2005). Quality assessment for geo-spatial objects derived from remotely sensed data. *International Journal of Remote Sensing, 26*(14), pp 2953 - 2974.

Zhang, Y. J. (1996). A survey on evaluation methods for image segmentation. *Pattern Recognition, 29*(8), 1335-1346.

Zhengrong, L., Hayward, R., Jinglan, Z., & Yuee, L. (2008). *Individual tree crown delineation techniques for vegetation management in power line corridor*. Paper presented at the 2008 Digital Image Computing: Techniques and Applications, 1-3 Dec. 2008, Piscataway, NJ, USA.

APPENDICES

Appendix 1: Plot information of the study area

Plot No.	Dominant Species	Mean DBH cm	Mean Height m	Aspect	Slope %	Altitude m	Crown Cover %
1	*Alnus nepalensis*	15	16	NE	15	1569	75
2	*Alnus nepalensis*	15	13	NE	20	1871	60
3	*Alnus nepalensis*	26	17	EN	70	1596	50
4	*Alnus nepalensis*	15	12	NE	35	1821	60
5	*Alnus nepalensis*	22	15	WN	70	1571	60
6	*Alnus nepalensis*	23	15	EN	0	1241	70
7	*Alnus nepalensis*	25	14	NW	70	1353	75
8	Alnus-Schima	18	8	EN	20	1692	40
9	Pinus species	33	20	EN	20	1393	50
10	Pinus species	21	17	EN	25	1949	65
11	Pinus species	30	17	EN	70	1765	50
12	Pinus species	27	20	EN	35	1485	85
13	Pinus species	23	15	EN	35	1601	60
14	Pinus species	29	20	ES	20	2107	65
15	Pinus species	29	20	EN	25	1443	80
16	Pinus species	19	15	EN	15	1394	50
17	Pinus species	20	13	EN	60	1678	60
18	Schima walichii	18	14	NE	15	1811	75
19	Schima - other BL	13	14	EN	35	1710	45
20	Schima - other BL	17	11	NW	25	1555	80
21	Schima-Alnus	15	12	NW	50	1766	60
22	Schima-Alnus	21	17	NW	5	1670	85

Appendix 2 Sampling plots in CFUGs of Dolakha

SN	Name of CF	Sample taken (by ICIMOD)	Sample in field
1	Charnawati_02	1	1
2	Charnawati_01	1	0
3	Bhitteri	2	0
4	Seti Devi	4	0
5	Botle Setidevi	1	1
6	Dhande Singhadevi	5	0
7	Sankha Devi	2	0
8	Thangsa Deurali	4	0
9	Majhkharka Lisepani	2	0
10	Napke Yanmara	1	1
11	Thumka Danda	1	1
12	Timure Tinsalle	0	2
13	Eklepakha	2	0
14	Shivajang Bhumesthan	0	2
15	Bhasmepakha	0	1
16	Dimal	0	2
17	Bhirmuni Devithan	0	2
18	Kupri Salleri	1	1

19	Paleko Ban	0	2
20	Chuche Dhungha	0	2
21	Devithan	1	1
22	Simpani	1	0
23	Pauwa	1	1
24	Tharlange	2	0
25	Dhande	0	2
26	Mahabhir	0	2
27	Chyase Bhagabati	0	2
28	Pokhari	0	2
29	Ramite	0	2
30	Bhakare	0	2
31	Mathani	0	2
32	Amlekharka	0	1
33	Mahankal	0	2
34	Harisiddhimai	0	2
35	Gahate Baghkhor	0	2
36	Barkhe Dandapari	0	2
37	Salleri	2	0
38	Simsungure	1	1
39	Palung Mahila	0	2
40	Chhitakunda	0	0
41	Sundari Mai	0	2
42	Bichaur	0	2
43	Kopila	0	2
44	Bhudha Bhimsen	1	1
45	Golmeswor	2	0
46	Chyane Danda	1	1
47	Kamalamai	1	1
48	Thutemane	0	2
49	Sitakunda	1	1
50	Jyamire	0	0
51	Juge Darkha	1	1
52	Laligurans	0	1
53	Lodini	0	0
54	Sano Botle	1	1
55	Kalchhe	0	2
56	Srijana	2	0
57	Gothpani	1	1
58	Gairi Jungle	2	0
	Total	**48**	**64**

Appendix 3 Selected CF for subset

SN	Name of CF	Sample taken (by ICIMOD)	Sample in field	Area of CF (ha.)
1	Shivajang Bhumesthan	0	2	46,67
2	Bhasmepakha	0	1	10,93
3	Bhirmuni Devithan	0	2	5,98
4	Kupri Salleri	1	1	42,03
5	Chuche Dhungha	0	2	8,90
6	Devithan	1	1	43,94
7	Dhande	0	2	29,17
8	Chyase Bhagabati	0	2	30,32
9	Mathani	0	2	28,28
10	Amlekharka	0	1	6,60
11	Mahankal	0	2	39,38
12	Gahate Baghkhor	0	2	5,54
	Total	**2**	**20**	**297,76**

Appendix 4 The dataset of Study Area for Needle leaved tree species:

SN	Species	Height m	DBH cm	CPA Seg m^2	CPA Vis m^2	Total Biomass kg.	Carbon kg.
1	Pinus species	18	30	12	33,61	286,08	134,46
2	Pinus species	18	33	41,75	20,36	367,85	172,89
3	Pinus species	16	33	10,5	19,08	367,85	172,89
4	Pinus species	21	39	21	23,79	571,96	268,82
5	Pinus species	16	33	47,25	26,78	367,85	172,89
6	Pinus species	24	48	33,75	35,49	991,27	465,90
7	Pinus species	21	48	36,25	36,85	991,27	465,90
8	Pinus species	32	44	36,25	28,62	787,11	369,94
9	Pinus species	28	39	28	37,69	571,96	268,82
10	Pinus species	26	41	23,75	26,12	652,88	306,85
11	Pinus species	28	40	22,75	20,86	611,58	287,44
12	Pinus species	28	44	35,25	33,33	787,11	369,94
13	Pinus species	30	48	30,25	38,43	991,27	465,90
14	Pinus species	20	31	32	31,1	311,92	146,60
15	Pinus species	18	38	20,5	29,89	533,99	250,98
16	Pinus species	19	38	27,5	28,54	533,99	250,98
17	Pinus species	25	40	55	36,46	611,58	287,44
18	Pinus species	30	45	48,25	38,16	835,40	392,64
19	Pinus species	28	56	61	28,6	1492,41	701,43
20	Pinus species	30	43	28,5	32,99	740,62	348,09
21	Pinus species	30	39	26,75	24,34	571,96	268,82
22	Pinus species	21	41	21,25	24,87	652,88	306,85
23	Pinus species	22	30	15,25	34,96	286,08	134,46
24	Pinus species	5	34	18	18,34	398,02	187,07
25	Pinus species	23	42	32	25,46	695,88	327,06
26	Pinus species	21	27	28,5	20,4	216,75	101,87

27	Pinus species	21	34	16,75	20,83	398,02	187,07
28	Pinus species	22	34	37,5	22,62	398,02	187,07
29	Pinus species	20	33	12,75	13,66	367,85	172,89
30	Pinus species	22	29	9,25	14,69	261,63	122,97
31	Pinus species	25	48	26,75	43,45	991,27	465,90
32	Pinus species	27	43	34,75	45,74	740,62	348,09
33	Pinus species	20	23	25,25	17,9	142,19	66,83
34	Pinus species	21	49	52	41,98	1046,99	492,08
35	Pinus species	18	41	27,75	41,98	652,88	306,85
36	Pinus species	8	16	17	9,19	54,95	25,83
37	Pinus species	17	38	38,75	20,99	533,99	250,98
38	Pinus species	8	18	19,75	4,53	74,77	35,14
39	Pinus species	10	21	12,25	11,02	111,98	52,63
40	Pinus species	14	26	13	18,52	196,26	92,24
41	Pinus species	25	33	11	26,63	367,85	172,89
42	Pinus species	13	29	30,25	15,46	261,63	122,97
43	Pinus species	17	54	35	42,9	1354,99	636,84
44	Pinus species	24	47	68,25	41,57	937,45	440,60
45	Pinus species	25	32	16,75	11,58	339,17	159,41
46	Pinus species	29	42	30,75	42,92	695,88	327,06
47	Pinus species	12	26	20	13,47	196,26	92,24